THE EFFECT OF THE TREATMENT WITH VARIOUS LIPID SPECIES ON MITOCHONDRIAL AND CELLULAR FUNCTIONS OF HEPATOCYTES

by

Peter Masschelin

A Thesis
Submitted to the
Graduate Faculty
of
George Mason University
in Partial Fulfillment of
The Requirements for the Degree
of
Master of Science
Biology

Committee:

_____	Dr. Ancha Baranova, Thesis Director
_____	Dr. Aybike Birerdinc, Committee Member
_____	Dr. Karl Fryxell, Committee Member
_____	Dr. Iosif Vaisman, Acting Director, School of Systems Biology
_____	Dr. Donna M. Fox, Associate Dean, Office of Student Affairs & Special Programs, College of Science
_____	Dr. Peggy Agouris, Dean, College of Science
Date: _____	Summer Semester 2017 George Mason University Fairfax, VA

The Effect of the Treatment with Various Lipid Species on Mitochondrial and Cellular Functions of Hepatocytes

A Thesis submitted in partial fulfillment of the requirements for the degree of Master of Science at George Mason University

by

Peter Masschelin
Bachelor of Science
Allegheny College, 2014

Director: Ancha Baranova, Professor
School of Systems Biology

Summer Semester 2017
George Mason University
Fairfax, VA

DEDICATION

This is dedicated to my mentors and coworkers who have always provided unwavering support.

ACKNOWLEDGEMENTS

I would first like to thank my advisor, Dr. Baranova, for her support and help in completion of this project. I would also like to thank Dr. Rohini Mehta, Dr. J. Michael Estep, and Dr. Aybike Birerdinc for their help and guidance as well as their continued support.

TABLE OF CONTENTS

Page
List of Tables viii
List of Figures ix
List of Equations xi
List of Abbreviations xii
Abstract xv
Chapter One: Non-Alcoholic Fatty Liver Disease 1
1.1 Prevalence and Etiology of NAFLD 1
Chapter Two: Fatty Acids and Their Biological Roles 3
2.1 Fatty Acid Classification 3
2.2 Storage of Fatty Acids in Triacylglycerols and Lipid Droplets 4
2.3 Translocation of Fatty Acids Across the Plasma Membrane 5
2.4 Mitochondrial Fatty Acid Import and Breakdown 6
2.5 β-Oxidation in the Mitochondria 7
2.6 Lipogenesis 9
2.7 Altered Lipid Contents in NAFLD Livers 10
2.8 Diet-Induced NAFLD/NASH in Rodents 12
2.9 Gene Expression Changes upon the Change in Lipid Intake 13
2.10 Regulation of Mitochondrial Activity 14
Chapter Three: Study Design and Methods 17
3.1 Specific Aims 17
3.2 Methods 17
3.2.1 Cell Culturing 17
3.2.2 Cell Viability and Seeding Density 18
3.2.3 Fatty Acid Treatments 19
3.2.4 Cell-based Assays 21
3.2.5 DNA Extraction, Purification, and Quantification 23

3.2.6 RNA Extraction 28
3.2.8 cDNA Synthesis 29
3.2.9 Evaluation of Mitochondrial Homeostasis and Lipid Processing Genes by qPCR 29
Chapter Four: Results 31
4.1 Study Design 31
4.2 A study of Lipid Accumulation in HepG2 cells Exposed to Oleic, Palmitic, or Butyric acids 32
4.2.1 Time Course of Lipid Accumulation in Response to the Treatment with Palmitic, Oleic or Butyric Acids 32
4.2.2 Lipid Accumulation is Altered in HepG2 Cells Exposed to Either 800uM or 250uM Butyric Acid 37
4.3 A Study of Changes in the Ratio of Mitochondrial to Nuclear DNA in HepG2 cells Exposed to Palmitic, Oleic or Butyric Acids 38
4.3.1 Time Course Changes in the Ratio of Mitochondrial to Nuclear DNA in Response to the Treatment with Palmitic, Oleic or Butyric Acids 38
4.3.2 Changes in Lipid Concentration Resulted in No Changes in the Ratio of Mitochondrial to Nuclear DNA Following Exposure to Oleic, Palmitic, or Butyric Acid 42
4.4 Apoptosis 43
4.6 Changes in the Levels of mRNAs Encoding Genes Involved in Mitochondrial Homeostasis and Lipid Processing 43
4.6.1 Effects of Oleic acid on Expression of Various Genes Involved in Lipid Metabolism and Mitochondrial Homeostasis 44
4.6.1.1 CPT-1a mRNA Levels Were Altered in Response to Changes in Oleic Acid Concentration, but not to Time 44
4.6.1.2 TFAM mRNA Levels were Altered in Response to Varying Concentrations of Oleic Acid 47
4.6.1.3 Exposure to Oleic Acid Significantly Alters CPT-1a and TFAM mRNA Levels 48
4.6.2 Effects of Palmitic Acid on Expression of Various Genes Involved in Lipid Metabolism and Mitochondrial Homeostasis 49
4.6.2.1 Exposure to Palmitic Acid Alters CPT-1a mRNA Levels 49
4.6.2.2 ACOX1 mRNA Levels were Altered in Response to Exposure Duration of Palmitic Acid 52
4.6.2.3 MFn2 mRNA Levels were Altered in Response to Palmitic Acid 53

4.6.2.4 Palmitic Acid Exposure Concentration Significantly Alters CPT-1a and MFn2 mRNA Levels 54
4.6.3 Effects of Butyric acid on Expression of Various Genes Involved in Lipid Metabolism and Mitochondrial Homeostasis 55
4.6.3.1 Butyric Acid Exposure Duration and Concentration Both Alter ACADM mRNA Levels 56
4.6.3.2 Butyric Acid Exposure Duration Alters ACOX1 mRNA Levels 59
4.6.3.3 Butyric Acid Exposure Duration and Concentration Both Altered PPARGC1A mRNA Levels 61
4.6.3.4 Butyric Acid Exposure Duration and Concentration Altered TFAM mRNA Levels 63
4.6.3.5 Butyric Acid Exposure Concentration Significantly Alters ACADM and PPARGC1A mRNA Levels 65
Chapter Five: Discussion 66
5.1 Exposure to Fatty Acids May Influence Lipid Metabolism 66
5.2 Effects of Exposure to Fatty Acids on the Ratio of Mitochondrial to Nuclear DNA and Oxidative Stress 70
References 78

LIST OF TABLES

Table Page
Table 1: Primer Sequences..... 27
Table 2: The Results of Oleic Acid Lipid Accumulation Assay 33
Table 3: The Results of an Assay of Palmitic Acid Dependent Lipid Accumulation. 34
Table 4: The Results of an Assay for Butyric Acid Dependent Lipid Accumulation. 36
Table 5: The Fold Changes in Lipid Accumulation Following the Treatment with Butyric Acid. 36
Table 6: The Effects of Exposure to Oleic acid on the Ratio of Mitochondrial to Nuclear DNA 39
Table 7: The Effects of the Exposure to Palmitic Acid on the Ratio of Mitochondrial to Nuclear DNA. 40
Table 8: The Effects of the Exposure to Butyric Acid on the Ratio of Mitochondrial to Nuclear DNA. 42
Table 9: The Changes in CPT-1a mRNA Levels Following Oleic Acid Treatment. 45
Table 10: Fold Change (Treated/Untreated) in mRNA Levels Following Exposure to Oleic Acid 46
Table 11: The Changes in TFAM mRNA Levels Following Oleic Acid Treatment..... 47
Table 12: The Changes in CPT-1a mRNA Levels Following Palmitic Acid Treatment.. 49
Table 13: Fold Change (Treated/Untreated) of mRNA Levels Following Exposure to Palmitic Acid 50
Table 14: The Changes in ACOX1 mRNA Levels Following Palmitic Acid Treatment. 52
Table 15: The Changes in MFn2 mRNA Levels Following Palmitic Acid Treatment. ... 54
Table 16: Fold Change (Treated/Untreated) of mRNA Levels Following Exposure to Butyric Acid..... 55
Table 17: The Changes in ACADM mRNA Levels Following Butyric Acid Treatment. 57
Table 18: The Changes in ACOX1 mRNA Levels Following Butyric Acid Treatment.. 59
Table 19: The Changes in PPARGC1A mRNA Levels Following Butyric Acid Treatment. 62
Table 20: The Changes in TFAM mRNA Levels Following Butyric Acid Treatment. ... 64
Table 21: Summary of Observations 75

LIST OF FIGURES

Figure Page
Figure 1: Progression of NAFLD to Cirrhosis 1
Figure 2: Representative Fatty Acid Species: a) Short Chain (C4 Butyric Acid), ... 4
Figure 3: 1 Round of Mitochondrial Beta-Oxidation of an Even-Numbered Saturated Fatty Acid 9
Figure 4: PPARGC1A as a Master Regulator: 16
Figure 5: Study Design 31
Figure 6: The Results of an Assay for Oleic Acid Induced Lipid Accumulation. 33
Figure 7: The Results of an Assay of Palmitic Acid Induced Accumulation of Lipid. 35
Figure 8: The Results of Butyric Acid-induced Lipid Accumulation Assay. 37
Figure 9: The Effects of Exposure to Oleic Acid on the Ratio of Mitochondrial to Nuclear DNA. 39
Figure 10: The Effects of Exposure to Palmitic Acid on the Ratio of Mitochondrial to Nuclear DNA. 41
Figure 11: The Effects of Exposure to Butyric Acid on the Ratio of Mitochondrial to Nuclear DNA. 42
Figure 12: The Changes in CPT-1a mRNA Levels Following Oleic Acid Treatment. 45
Figure 13: The Changes in TFAM mRNA Levels Following Oleic Acid Treatment. 48
Figure 14: The Changes in CPT-1a mRNA Levels Following Palmitic Acid Treatment. 50
Figure 15: The Changes in ACOX1 mRNA Levels Following Palmitic Acid Treatment. 53
Figure 16: The Changes in MFn2 mRNA Levels Following Palmitic Acid Treatment. .. 54
Figure 17: The Changes in ACADM mRNA Levels Following Butyric Acid Treatment. 58
Figure 18: Pairwise Comparison of ACADM mRNA Levels Following Exposure to 250uM Butyric acid 58
Figure 19: The Changes in ACOX1 mRNA Levels Following Butyric Acid Treatment. 60
Figure 20: Pairwise Comparison of ACOX1 mRNA Levels Following Exposure to 800uM Butyric acid 60
Figure 21: The Changes in PPARGC1A mRNA Levels Following Butyric Acid Treatment. 62
Figure 22: Pairwise Comparison of PPARGC1A mRNA Levels Following Exposure to 800uM Butyric Acid 63
Figure 23: The Changes in TFAM mRNA Levels Following Butyric Acid Treatment. .. 64
Figure 24: Pairwise Comparisons of TFAM mRNA Levels Following Exposure to 250uM Butyric acid 65

Figure 25: The Dynamic Metabolic Control of PPARα and PPARGC1α. 68
Figure 26: Fatty Acid Species used in this Assay: 75

LIST OF EQUATIONS

Equation Page
Equation 1: Dilution of Butyric acid..... 20

LIST OF ABBREVIATIONS

3-Hydroxy-3-Methylglutaryl-Coenzyme A Synthase 1 ..... HMGCS1
Acyl-CoA Dehydrogenases ..... ACAD
Adenosine Triphosphate ..... ATP
AMP-Activated Protein Kinase ..... AMPK
Analysis of Variance ..... ANOVA
Beta-2 Microglobulin B2M
Beta-Actin ..... ACTB
B-ketoacyl CoA Reductase ..... KCR
B-Ketoacyl CoA Synthase ..... KCS
Butyric acid ..... BA
Carboxylesterase 2 ..... Ces2
Carnitine AcetylTransferase ..... CRaT
Carnitine Acyl-Transferase ..... CAT
Carnitine Octanoyltransferase ..... COT
Carnitine Palmitoyl Transferase ..... CPT
Carnitine Palmitoyltransferase 1A CPT-1a
Chromatin Immunoprecipitation ..... ChIP
Coenzyme A ..... CoA
Complementary DNA ..... cDNA
Cytokeratin 18 ..... CK18
Deoxyribonucleic Acid ..... DNA
Diacylglycerol ..... DAG
Dimethyl Sulfoxide ..... DMSO
DNA Methyltransferase ..... DNMT
Docosahexanoic Acid ..... DHA
Double Distilled Water ..... ddH_2O
Dulbecco's Modified Eagle Medium/Nutrient Mixture 12 ..... DMEM/F12
Eicosapentaenoic Acid ..... EPA
Enzyme-Linked Immunosorbent Assay ..... ELISA
Fatty Acid Desaturase ..... FADS
Fatty Acid Synthase ..... FAS
Fatty Acid Transport Protein ..... FATP
Fetal Bovine Serum ..... FBS
Flavin Adenine Dinucleotide ..... FAD
Fold Change ..... FC
Horseradish Peroxidase ..... HRP

Hydrogen Peroxide ..... H_2O_2
Hypervariable Segment ..... HVS
Lipoprotein Lipase 1 ..... Lp1
Long Chain Acyl-CoA Dehydrogenase ..... LCAD
Long Chain Fatty Acid ..... LCFA
Long-Chain Fatty Acid ..... LCFA
Matched Untreated 250uM U2
Matched Untreated 800uM U1
Mean Difference ..... MD
Medium Chain Acyl-CoA Dehydrogenase ..... MCAD
Medium Chain Fatty Acid ..... MCFA
Methionine-Choline Deficient ..... MCD
Methyl-Deficient Diet ..... MDD
Mitochondrial DNA ..... mtDNA
Mitochondrial NADH Dehydrogenase 6 ..... MT-ND6
Mitochondrial Transcription Factor A ..... TFAM
Mitofusin-2 ..... Mfn2
Monounsaturated Fatty Acid ..... MUFA
Nicotinamide Adenine Dinucleotide Phosphate ..... NADP
Nicotinamide Adenine Dinucleotide ..... NAD
Non-Alcoholic Fatty Liver Disease ..... NAFLD
Non-Alcoholic Steatohepatitis ..... NASH
Nuclear DNA ..... nDNA
Oil Red O ..... ORO
Oleic acid ..... OA
Palmitic acid ..... PA
Patatin like Phospholipase Domain Containing ..... PNPLA
Penicillin/Streptomycin ..... P/S
Peroxisomal Acyl-Coenzyme A Oxidase 1 ..... ACOX1
Peroxisome Proliferator-Activated Receptor Gamma Coactivator-1 Alpha PPARGC1A
Phosphate Buffered Saline ..... PBS
Phosphatidylserine ..... PS
Polymerase Chain Reaction ..... PCR
Polyunsaturated Fatty Acid ..... PUFA
Quantitative Polymerase Chain Reaction ..... qPCR
Reactive Oxygen Species ..... ROS
Real-time Polymerase Chain Reaction ..... rtPCR
Ribonucleic Acid ..... RNA
Saturated Fatty Acid ..... SFA
Short Chain Acyl-CoA Dehydrogenase ..... SCAD
Short Chain Fatty Acid ..... SCFA
Standard Deviation ..... SD
Sterol-C4-Methloxidase-Like SC4MOL
Steroyl-Coenzyme A Desaturase 2 ..... Scd2

Tergitol-Type NP-40 ..... NP-40
Treated 250uM C2
Treated 800uM C1
Triacylglycerol ..... TAG
Very Long Chain Acyl-CoA Dehydrogenase ..... ACADVL
Very Long Chain Fatty Acid ..... VLCFA
Very Low Density Lipoprotein ..... VLDL

ABSTRACT

THE EFFECT OF THE TREATMENT WITH VARIOUS LIPID SPECIES ON MITOCHONDRIAL AND CELLULAR FUNCTIONS OF HEPATOCYTES

Peter Masschelin, M.S.

George Mason University, 2017

Thesis Director: Dr. Ancha Baranova

Non-alcoholic fatty liver disease (NAFLD) is a growing epidemic characterized by increased intrahepatic lipid accumulation. In some individuals, NAFLD progresses to non-alcoholic steatohepatitis (NASH), with complications including hepatocellular carcinoma and cirrhosis. As a rise in NAFLD cases has been associated with an increase in the consumption of high levels of fats and carbohydrates, also known as a high-caloric diet, and in obesity, understanding how dietary fatty acids contribute to the development of NAFLD through their effects on mitochondrial biogenesis and fatty acid oxidation may expand an array of potential therapeutics for the treatment of NAFLD. In this study, hepatocytes were treated with two concentrations (800uM and 250uM) of dietary fatty acids (oleic, palmitic, and butyric). These treatments resulted in changes in lipid accumulation, the ratio of mitochondrial to nuclear DNA, and the levels of expression of mRNAs involved in mitochondrial homeostasis and lipid processing. Interestingly, oleic

and palmitic acids, although both classified as long-chain fatty acids, did not have the same effect on those cellular characteristics. Specifically, treatment with either 800uM or 250uM of oleic acid resulted in a decrease in *CPT-1a* expression, suggesting a decrease in mitochondrial fatty acid import. In comparison, treatment with 800uM palmitic acid resulted in a significant increase in *CPT-1a* expression, suggesting an increase in mitochondrial fatty acid import. Palmitic acid also induced increased expression of *ACOX1* and *MFn2* suggesting increased peroxisomal beta-oxidation and reorganization of the mitochondrial architecture. Exposure to a short chain fatty acid, butyrate, resulted in lipid accumulation, changes in expression pattern of genes involved in beta-oxidation, and no change in the ratio of mitochondrial to nuclear DNA. Overall, this study profiled the dynamic and complex responses of hepatocytes to exogenous free fatty acids. Differences in expression levels of genes involved in beta-oxidation brings some insight into a dynamic interplay of fatty acids, their breakdown by beta-oxidation, and transcriptional regulation in human hepatocytes in response to fatty acids.

CHAPTER ONE: NON-ALCOHOLIC FATTY LIVER DISEASE

1.1 Prevalence and Etiology of NAFLD

Non-alcoholic fatty liver disease (NAFLD) is a chronic metabolic disorder characterized by the presence of hepatic steatosis without a secondary cause of hepatic fat accumulation (Chalasani et al., 2012). Initially, the term "NAFLD" was coined at the May Clinic by Dr. Jurgen Ludwig, following identification of 20 moderately obese individuals with nonalcoholic steatohepatitis (NASH) of unknown causes with the presence of lobular hepatitis, fibrosis in most cases, and, in three individuals, even cirrhosis (Ludwig et al., 1980). Steatosis is defined as marked intrahepatic lipid accumulation. NAFLD is a potential progressive disease as it can advance to non-alcoholic steatohepatitis (NASH), with complications including hepatocellular carcinoma (Figure 1).

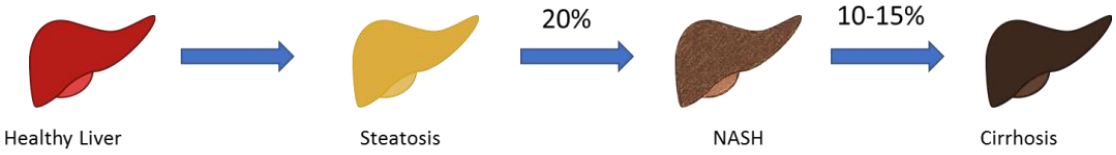

Figure 1: Progression of NAFLD to Cirrhosis

Global estimates for the presence of NAFLD are far from being perfect. According to available surveys, NAFLD has an estimated world-wide prevalence of 25.24% with higher rates in South America and the Middle East and lower rates in Africa (Younossi et al., 2016). Comparison of populations in the United States revealed different prevalence rates in different ethnic groups with a higher prevalence of hepatic steatosis in Hispanic individuals and a positive correlation with obesity and insulin resistance (Browning et al., 2004). In individuals of African descent, the prevalence of hepatic steatosis is lower, and has no correlation to obesity and insulin resistance (Browning et al., 2004). While the mechanism for NAFLD has not been fully elucidated, both genetics and diet play an important role in its progression. Increased consumption of fatty acids, leading to increase in plasma levels of free fatty acids (FFA), has been associated with NAFLD, but the mechanisms of this pathophysiological phenomenon are not fully understood.

CHAPTER TWO: FATTY ACIDS AND THEIR BIOLOGICAL ROLES

2.1 Fatty Acid Classification

Lipids encompass a vast group of active biomolecules and include prenol lipids, fatty acids, glycerolipids, sphingolipids, sterols, and others (Fahy et al., 2009; Fahy et al., 2011). Fatty acids (FAs) are composed of a carboxylic head attached to a hydrocarbon tail with varying lengths and degrees of saturation. FAs vary in length, the most common fatty acids containing 12-22 carbon atoms (Rustan and Drevon, 2001). Long-chain FAs can be saturated or unsaturated (monounsaturated (MUFA), or polyunsaturated (PUFA)), with each class having a plethora of biological roles (Figure 1). As their name suggests, monounsaturated fatty acids contain one double bond while polyunsaturated fatty acids may contain 2 or more. Fatty acids can further be classified by their length including short chain (SCFA), medium chain (MCFA), long chain (LCFA), and very long chain (VLCFAs). SCFAs typically contain 5 or fewer carbon units, with MCFAs containing 6-12 carbon units, LCFAs containing 13-21 carbon units, and VLCFAs containing more than 22 carbon units. In animal tissues, saturated fatty acids (SFA) are around 30-40% of the total fatty acid content with 15-25% of those being palmitic acid, 10-20% being stearic acid, and 0.5-1% being myristic acid (Legrand and Rioux, 2010).

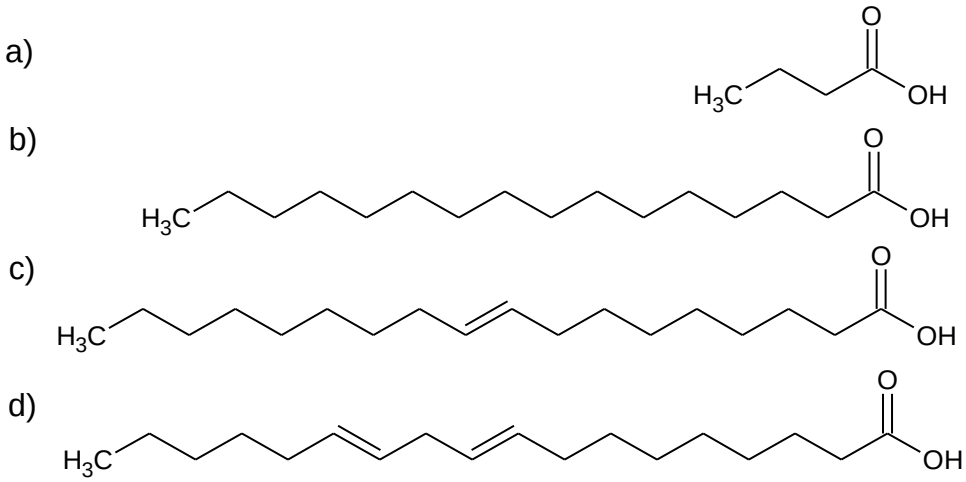

Figure 2: Representative Fatty Acid Species: a) Short Chain (C4 Butyric Acid), b) Unsaturated (C16 Palmitic acid), c) Monounsaturated (C18:1 Oleic acid), d) Polyunsaturated (C18:2 Linoleic acid).

2.2 Storage of Fatty Acids in Triacylglycerols and Lipid Droplets

Fatty acids can exist as free fatty acids (FFAs) or could be bound in complexes as in the case of triacylglycerols (TAG) and diacylglycerols (DAG), and phospholipids. Triacylglycerols are composed of a glycerol backbone to which three fatty acid molecules are attached. These FAs can be the same or different species leading to n^3 possible enantiomers, where n represents number of fatty acid species present (Mu and Høy, 2004). Experimental evidence with 3T3-L1 cells incubated with acetate, myristate, palmitate, stearate, and oleate revealed that triglyceride enrichment with saturated fatty acids results in preferential esterification at the sn-1 or sn-3 position while enrichment with unsaturated fatty acids results in preferential esterification at the sn-2 position (Ahmadian et al., 2007; Soma et al., 1992). The sn position is the position in the triglyceride molecule with sn-2 being the middle position.

In the human diet, TAGs containing LCFAs account for 95% of dietary fatty acids (Niot et al., 2009). During times of high energy demands, these TAGs are then converted to DAGs and free fatty acids. Typically, lipids are not stored as fatty acids, but are esterified to produce TAGs and packaged in to cytoplasmic lipid droplets for storage (Aon et al., 2014). TAG accumulation may also provide a protective effect against lipotoxicity from saturated fatty acids as oleic acid (C18:1) was readily incorporated into TAGs while palmitic acid (C16) was not well incorporated and induced apoptosis in Chinese Hamster Ovary (CHO) cells (Listenberger et al., 2003). Increased levels of TAGs have been associated with high levels of atherogenic lipoproteins, particularly in individuals with metabolic syndrome and type 2 diabetes (Talayero and Sacks, 2011).

2.3 Translocation of Fatty Acids Across the Plasma Membrane

Release of fatty acids from cells requires their cleavage from TAGs followed by binding to serum albumin for transportation. Consequently, incorporation of fatty acids into cells requires many steps including the dissociation from serum albumin or intestinal micelles, plasma membrane transport, binding to intracellular proteins, and/or esterification to acyl-CoAs (Ehehalt et al., 2006). This translocation includes both simple diffusion and a highly regulated saturable transport process (Ehehalt et al., 2006). While the process for diffusion requires no additional proteins, a group of fatty acid transport proteins (FATPs), encoded by the *SLC17* gene family, have been heavily implicated in the active transport process (Faergeman et al., 1997).

The *SLC27* gene family comprises six members, *SLC27A1-6*, which encode fatty acid transport proteins FATP1-6. It has been proposed that FATPs assist in the transport

of long-chain fatty acids across the plasma membrane. Evidence in favor of the involvement of FATPs in active fatty acid transport includes identification of a cDNA encoding a protein with six membrane-spanning regions and its localization to the plasma membrane (Schaffer and Lodish, 1994). The genome of *Saccharomyces cerevisiae* contains the gene (*FAT1*) which encodes a protein that shares 33% sequence similarity to the *SLC27A1*-encoded protein FATP1, previously identified in 3T3-L1 adipocytes by Schaffer and Lodish; with the disruption of this yeast protein resulted in impaired growth in the presence of fatty acids and a decrease in the uptake of fluorescently labelled fatty acids. More recent research has shown that targeted deletion in FATP5 resulted in decreased triglyceride and FFA content, while overexpression increased the uptake of oleate, indicating that fatty acid transport proteins play a larger role in lipid homeostasis than previously thought (Doege et al., 2006).

2.4 Mitochondrial Fatty Acid Import and Breakdown

There are many possible fates for fatty acids following import into the cytoplasm including storage in lipid droplets or breakdown in the mitochondria. Import of fatty acids into the mitochondria depends on the chain length as LCFAs are unable to pass through the inner mitochondrial membrane, thus activation on the outer membrane by long-chain acyl-CoA synthetase is necessary (See Kerner and Hoppel, 2000 for review). Carnitine acyltransferases (CAT), which are required in the transport of fatty acids into the mitochondria, catalyze the transfer of an acyl group to carnitine from acyl-CoA. CATs can be divided into three categories: 1) carnitine palmitoyl transferases (CPTs), which preferentially transfer medium and long chain fatty acids, 2) carnitine

octanoyltransferases (COT), which transfer both medium and long chain fatty acids, and 3) carnitine acetyltransferases (CrAT) which convert acetyl-CoA to acetyl-carnitine in the mitochondrial matrix (See Sharma and Black, 2009 for review).

CPT-1 and CPT-2 are used for the transfer of long-chain fatty acids, such as oleic acid and palmitic acid, into the mitochondrial matrix. CPT-1 regulates the conversion of acyl-CoA to acyl-carnitine and is a site of beta-oxidation regulation as it is inhibited by malonyl-CoA (McGarry et al., 1978). Carnitine-acylcarnitine translocase transports the acylcarnitine across the inner mitochondrial membrane while transporting carnitine into the intermembrane space. In the mitochondrial matrix, CPT-2 converts the acylcarnitine back to acyl-CoA and free carnitine, which allows the fatty acid to be further broken down by beta-oxidation (See Kerner and Hoppel, 2000 for review).

2.5 β-Oxidation in the Mitochondria

Beta-oxidation is the process through which fatty acyl-CoA molecules are broken down, releasing acetyl-CoA which is then used by the electron transport chain to produce ATP. While β-oxidation occurs in both the mitochondria and peroxisomes, dicarboxylic and very long-chain monocarboxylic fatty acids are only used in the peroxisomal pathway (Poirier et al., 2006).

In the mitochondria, beta-oxidation occurs as a 4-step cycle including dehydrogenation, hydration, oxidation, and thiolysis. This results in two-carbon acetyl-CoA units being released after every cycle. This cycle is altered in the case of odd-numbered fatty acids or if the acyl-CoA is desaturated. In the case of a long-chain acyl-

CoA, after entry into the mitochondria, members of the acyl-CoA dehydrogenase (ACAD) family provide the first step. The ACAD enzyme used differs depending on the length of the acyl-CoA, with very long chain acyl-CoA dehydrogenase (ACADVL), long chain acyl-CoA dehydrogenase (ACADL), medium chain acyl-CoA dehydrogenase (ACADM), and short chain acyl-CoA dehydrogenase (ACADS) acting on their respective acyl-CoA molecules (See Houten and Wanders, 2010 for review). The second step requires the enzyme enol-CoA hydratase and the presence of water, resulting in the hydration of the double bond formed by the first step. The third step requires the cofactor NAD^+ and the enzyme 3-hydroxyacyl-CoA dehydrogenase to dehydrogenate the acyl-CoA. The fourth step involves the cleavage of an acetyl-CoA group from the acyl-CoA molecule in the presence of CoA-SH and the enzyme 3-ketoacyl-CoA thiolase. Each cycle of oxidation also yields one molecule of $FADH_2$ and 1 molecule of NADH, which are used in a variety of processes including the electron transport chain (See Houten and Wanders, 2010 for review) (Figure 3).

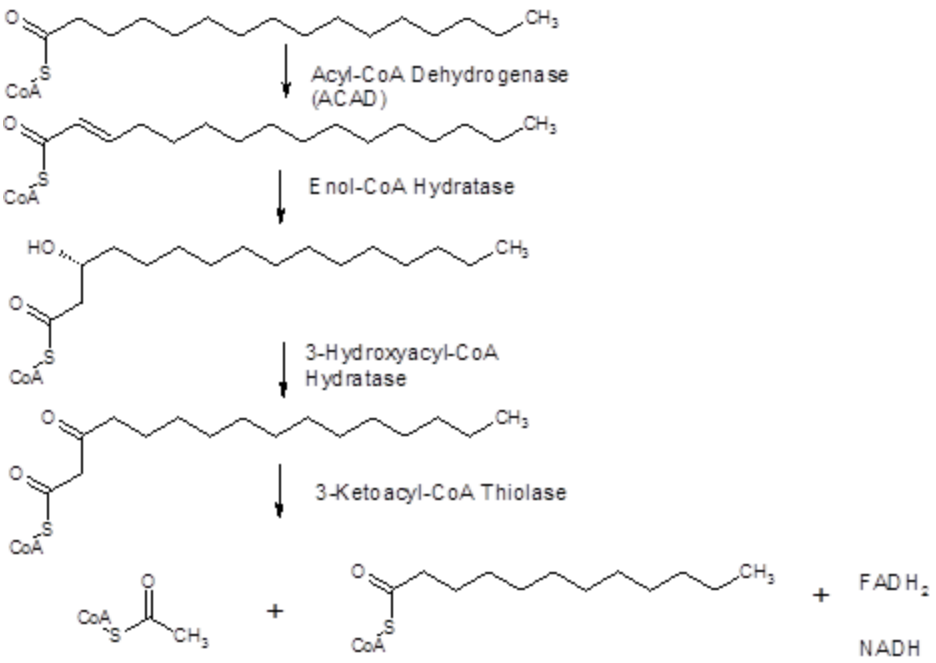

Figure 3: 1 Round of Mitochondrial Beta-Oxidation of an Even-Numbered Saturated Fatty Acid

2.6 Lipogenesis

Lipogenesis is a stepwise process where fatty acids are synthesized from excess carbohydrates, which can then be stored in TAGs for future energy demands (Ameer et al., 2014). Initial requirements for lipogenesis include the influx of the citrate which is produced by the citric acid cycle. Citrate is converted to acetyl-CoA by ATP-citrate lyase, and then to malonyl-CoA by acetyl-CoA carboxylase (See Lodhi et al., 2011 for review). Malonyl-CoA and acetyl-CoA bind to fatty acid synthase (FAS) in the presence of NADPH and elongation occurs through a repeated sequential process whereby the growing fatty acid is elongated by 2 carbon units per cycle, with the 2 carbon units being

supplied by malonyl-CoA (See Lodhi et al., 2011 for review). Modification of fatty acids, either produced through lipogenesis or ingested, includes desaturation and elongation. The steps and enzymes involved in the elongation process include: condensation by Beta-ketoacyl CoA synthase (KCS), reduction by Beta-ketoacyl CoA reductase (KCR), dehydration by Beta-hydroxyacyl CoA dehydrase, and reduction by trans-2-enoyl CoA reductase (Cinti et al., 1992; See Leonard et al., 2004 for review).

2.7 Altered Lipid Contents in NAFLD Livers

Increased intracellular lipid accumulation, which is known as steatosis, is a hallmark of NAFLD. Therefore, determination of the lipid composition and study of lipid species metabolism alterations is crucial to understanding of NAFLD and its treatment. Of the triacylglycerides (TAGs) accounted for in the liver in patients with NAFLD, 59% come from non-essential fatty acids, 26% from *de novo* lipogenesis, and 15% from the diet, supporting the hypothesis that accumulation of hepatic and lipoprotein fat in NAFLD is dependent both on elevated contents of the fatty acids in the diet and on *de novo* lipogenesis (Donnelly et al., 2005). Comparison of TAGs and free fatty acids in healthy and NAFLD individuals revealed that, in NAFL and NASH, total hepatic lipid contents are increased. Both TAGs and DAGs contents are increased, while the free fatty acid content remain unchanged (Puri et al., 2007).

In both an animal model for NAFLD and human NALFD patients, mass spectrometry analysis revealed evidence of modulation of Δ6-desaturase activity with decreased levels of linoleic acid and α-linoleic acids as well as increased levels of its

downstream product, arachidonic acid (Barr et al., 2010). When individuals with steatosis or cirrhosis were compared to controls, similar changes in phosphatidic acid were seen, while an increase in saturated and monounsaturated fatty acid containing phosphatidic acid species was notable (Gorden et al., 2011). For phospatidylserine (PS), the overall changes seen in steatotic and cirrhotic individuals as compared to controls were similar. In particular, a phosphatidylinositol species containing 38 carbon units and 4 double bonds (38:4 PI species) were increased in patients with steatosis, but decreased in patients with cirrhosis (Gorden et al., 2011). Altogether, a decrease in arachidonic acid-containing lipid species was noted across the majority of phospholipid classes in human liver specimens collected from patients with different stages of progressive disease, being especially prominent at the cirrhotic stage (Gorden et al., 2011). In plasma of individuals with simple steatosis or NASH, levels of phosphatidylinositol and phosphatidylserine were elevated compared to healthy controls, while levels of phosphatidylethanolamine were most elevated in NASH, followed by simple steatosis, and lowest in healthy controls (Ma et al., 2016).

Changes in the fatty acid composition of plasma phospholipids were also observed. In particular, increases in phosphatidylinositol and phosphatidylserine containing docosahexaenoic acids (DHA) were noted in individuals with NASH (5-fold) and simple steatosis (3-fold) compared to healthy controls. Levels of phosphatidylserine-containing arachidonic acid were higher in individuals with NASH and simple steatosis as compared to healthy controls, while levels of phosphatidylethanolamine-containing arachidonic acid were lower (Ma et al., 2016).

Comparison of the levels of diacylglycerols revealed multiple-fold increases in short chain (30-36 carbon atoms) species containing 0, 1, 2, ad 3 double bonds notable in human steatotic livers, but not in cirrhotic ones (Gorden et al., 2011). In steatotic livers, and in livers of NASH patients, increases in DAGs and TAGs contents were detected (Puri et al., 2007, 2009). In plasma, a significant decrease in stearic acid and an increase in oleic acid-containing DAGs was seen in both NAFL and NASH individuals (Puri et al., 2009).

2.8 Diet-Induced NAFLD/NASH in Rodents

Organismal models for NAFLD include nutritional and genetic models, with nutritional models playing a larger role. Nutritional models can be broken into two groups, one with increased lipid transport or synthesis in the liver, and another with decreased lipid export or catabolism (Kucera and Cervinkova, 2014). High-fat diets contain 50% of calories coming from fat, while healthy rodent diets contain less than 10% of fat calories (Fellmann et al., 2013). Mice on a diet providing 71% energy from fat, as compared to 35% in the control diet, develop NASH with all its the "classical" hallmarks, including steatosis, inflammation, and fibrosis (Lieber et al., 2004). Feeding mice a methyl-deficient diet (MDD) results in morphological changes similar to NASH, increased demethylation, decreased DNMT1 expression, and loss of H3K27 and H4K20 histone trimethylation, altering their hepatic epigenetic landscape (Pogribny et al., 2009). Other animal models include a deficiency in methionine and choline (MCD), which results in inflammation, hepatic fibrosis, a decrease in beta-oxidation, and a decrease in VLDL production (see Takahashi et al., 2012& Anstee and Goldin, 2006 for reviews).

2.9 Gene Expression Changes upon the Change in Lipid Intake

As NAFLD changes the lipidomic profile of individuals, alterations of gene expression patterns compensate for these changes. For example, profiling of 63 individuals who varied in the progression of NAFLD, led to identification of 22 gene signatures differentiating livers with simple steatosis and with NASH. The signature included genes involved in fatty acid desaturation, ether lipid metabolism, inflammatory pathways, detoxification, growth and development processes, and apoptosis (Arendt et al., 2015). Interestingly, individuals with NASH showed lower levels of hepatic long-chain polyunsaturated fatty acids, including that of biologically active eicosapentaenoic (EPA) and docosahexaenoic acids. Respectively, gene expression signature of NASH revealed enrichment for the genes of peroxisome proliferator-activated receptor signaling pathway, including *FADS1*, *FADS2*, and *PNPLA3* (Arendt et al., 2015)

In a rodent model of NASH, a high-fructose diet led to a decrease in Cyp7a1 expression, which is responsible for the rate limiting step in for the conversion of cholesterol into bile acids, suggesting that chronic, high-fructose consumption leads to increased accumulation of cholesterol (Renaud et al., 2014). In another study of NAFLD mice, a high-fat diet led to an increase in the expression of genes involved in lipid metabolism, including ones encoding lipoprotein lipase 1 (Lp1), stearoyl-Coenzyme A desaturase 2 (Scd2), carboxylesterase 2 (Ces2), and fatty acid synthase (Fasn). Down-regulation was observed for genes involved in cholesterol biosynthesis including 3-hydroxy-3-methyulglutaryl-coenzyme A synthase 1 (*Hmgcs1*) and sterol-c4-methyloidase-like (*Sc4mol*) (Wang et al., 2016). Pathway analysis highlighted high-fat

diet-related activation of lipid homeostasis, fatty acid uptake, lipid storage, inflammation, oxidative stress, and oxidoreductase activity, while the gene sets involved in nucleic acid and drug metabolism were downregulated (Wang et al., 2016). As lipid overload is a hallmark of NALFD, the upregulation of lipid metabolism genes is typically interpreted as an attempt to compensate for this overload.

2.10 Regulation of Mitochondrial Activity

Several endogenous and exogenous factors contribute to modulation of mitochondrial activity by altering either one or a combination of the following: mitochondrial DNA transcription, oxidative damage, reorganization of the mitochondrial architecture, and regulation of mitochondrial biogenesis. Mitochondrial transcription factor A (*TFAM*) is a transcription factor central in regulation of mtDNA copy number. *TFAM* is encoded in the nucleus and transported to the mitochondria where it plays a role in the regulation of mtDNA copy number. Heterozygous knockouts of *TFAM* decreased mtDNA copy number by 35-40%, while a homozygous knockout resulted in death.(Ekstrand et al., 2004; Larsson et al., 1998). Through the use of a mouse knockout model and *TFAM* overexpression, mitochondrial copy number was directly proportional to the level of TFAM in mice (Ekstrand et al., 2004).

Additionally, the close proximity of mitochondria to oxidative phosphorylation increases the risk for mitochondrial oxidative damage. Reactive oxygen species (ROS) generated during oxidative phosphorylation, can alter the mitochondrial DNA as well as reduce the efficiency in the mitochondria. To mitigate damaged mtDNA and/or mitochondria, reorganization of the mitochondrial architecture, through fusion and

fission, can be used as a "pro-survival" mechanism, (Barbour and Turner, 2014; Youle and van der Bliek, 2012). One such gene that plays an essential role in mitochondrial fusion is mitofusin-2 (*MFn2*).

A major regulator of mitochondrial biogenesis is peroxisome proliferator-activated receptor γ coactivator 1, PGC-*1α,* (encoded by *PPARGC1A*) (See Handschin and Spiegelman, 2006 for review). *PPARGC1A* is stimulated by, among other things, glucocorticoids and cAMP. *PPARGC1A* modulated by downstream genes are classified into 6 major ontologies, including Oxidative Phosphorylation, Protein Folding, Catabolic Processes, Lipid Metabolism, Stress Response, and Amino Acid Metabolism (Charos et al., 2012; Eynon et al., 2011; Gastaldi et al., 2007; Song et al., 2004) (Figure 4).

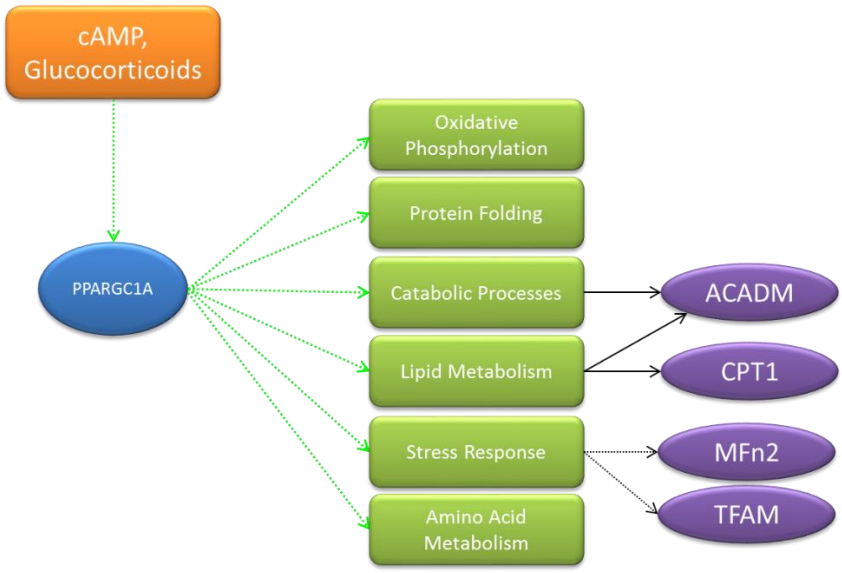

Figure 4: *PPARGC1A* as a Master Regulator: PPARGC1A response genes can be classified into 6 ontologies (green). Genes in purple belong in the ontology, are modulated by PPARGC1A, and are relevant to this study. Dashed lines indicate indirect modulation

CHAPTER THREE: STUDY DESIGN AND METHODS

3.1 Specific Aims

1. To analyze time-course changes in the lipid metabolism of HepG2 cells in response to their exposure to low (250uM) and high (800uM) concentrations of oleic acid, palmitic acid, and butyric acids by measuring intracellular lipid concentration and apoptosis/proliferation.
2. To determine mitochondrial response to exposure to oleic acid, palmitic acid, and butyric acids through determination of mtDNA/nDNA ratio and expression of genes involved in mitochondrial energy homeostasis

3.2 Methods

3.2.1 Cell Culturing

Immortalized hepatocellular carcinoma cells (HepG2) were grown and maintained in growth media (Dulbecco's Modified Eagle Medium/Nutrient Mixture F12 (DMEM/F12 1:1) (Hyclone) supplemented with 10% defined fetal bovine serum (FBS) (Hyclone) and 1% penicillin/streptomycin solution (Hyclone) in a humidified atmosphere with 5% CO_2 at 37°C. Cells were maintained at 70-80% confluent in 75 cm^2 vented cell culture flasks (Corning). Prior to trypsinization, the flasks were washed with pre-warmed 5mL PBS. Pre-warmed trypsin (Hyclone) 5mL was added to the flasks and incubated for 4 minutes at 37°C. To dislodge the trypsinized cells the flasks were gently rolled. HepG2

have a tendency to self-aggregate if agitated during trypsinization. To prevent cell clumping, cell confluence was maintained at less than 80% and trypsinization process was carried out by gently rolling the flask. At the end of incubation, trypsin was neutralized by addition of equal amounts of growth media (+10% FBS, +1% P/S). FBS contains protease inhibitors, which inactivate the trypsin. The cell suspension was centrifuged in a conical tube at 150g for 5 minutes. The supernatant was removed and the pellet re-suspended in 1mL growth media. Gentle pipetting with a 1ml pipette tip was carried out to prevent cell shearing. Viable cells were counted by trypan blue exclusion assay and seeded at desired density.

3.2.2 Cell Viability and Seeding Density

Viable cells were counted using trypan blue exclusion and automated cytometer (Countess, Thermo Fisher Scientific). The loss of membrane integrity was indicated by the entry of trypan blue dye (Invitrogen) into cells. Cell suspension of 10ul was diluted with equal volume of 0.1% trypan blue. The percentage of trypan-blue positive cells was calculated and the cells were seeded at desired cell count for the experiments. Care was taken to ensure uniform seeding density of cells across the plate by repeated pipetting the cell suspension, as the heavier cells have a tendency to settle down from suspension. For intracellular lipid accumulation study, cells were seeded at $5x10^4$ cells/well in 24-well plates. For DNA and RNA, cells were seeded at $6.75x10^5$ cells/well in 6-well plates. Prior to treatment, seeded cells were allowed to grow for 24 hrs in the culture vessel. Cells were then serum starved overnight in DMEM/F12 media with 1% penicillin/streptomycin to help synchronize the cells. At the end of overnight serum

starvation, the media was replaced with growth media and the desired treatments were carried out. The location of the treatment and control wells were randomized across the plate to compensate for variation in seeding density across wells. The controls and treatments were paired on the same plate to reduce variations and to ensure any variations in growth conditions were captured by the untreated controls.

3.2.3 Fatty Acid Treatments

Three types of fatty acids differing in degree of saturation and chain length were used in this study. Cells were treated with two different concentrations of each fatty acid: Low concentration (250uM) and High concentration (800uM). DMSO (Dimethyl Sulfoxide) was used to dissolve the non-polar fatty acids. Each type of cell treatment was compared with its untreated (no fatty acid) control. The changes in cell metabolism were assessed after exposure to treatment across a time course for 2, 4, 6, 12, and 24 hours. The DMSO concentration was kept constant across all treatments as well as in untreated controls to prevent effect of DMSO as a confounding factor. DMSO concentrations were kept below 0.5% to prevent cell toxicity. While preparing all stock and working solutions, cell growth media and free fatty acid solutions were preheated at 50˚C. When dispersing the treatment across plates, treatment solutions were mixed well to prevent separation.

Oleic acid: Oleic acid (cat # O1383, Sigma) was dissolved to 3.15M in DMSO. For a 50mM working solution, 15.8uL of preheated oleic acid stock (3.15M) was added to the pre-heated cell growth media for a molarity of 50mM. The 50mM solution was sonicated for 10 minutes at 100% amplitude with 10 seconds on and 1 second off. For the

final 1mM working solution, 0.7mL of 50mM solution was added to cell growth media to a final volume of 35mL.

$$\frac{\mathbf{0.2}\boldsymbol{mmol}}{\boldsymbol{mL}} * \mathbf{1}\boldsymbol{mL} * \frac{\mathbf{88.11}\,\boldsymbol{mg}}{\mathbf{1}\,\boldsymbol{mmol}} * \frac{\mathbf{1}\,\boldsymbol{\mu L}}{\mathbf{0.964}\,\boldsymbol{mg}}$$

Equation 1: Dilution of Butyric acid

Palmitic acid: 0.051g of pre-crushed Palmitic acid (≥99%, Sigma Aldrich cat # P0500) was dissolved in 1mL DMSO for a 200mM solution. To the pre-heated cell growth media, palmitic acid stock solution (250uL) was added for a molarity of 50mM. The 50mM solution was sonicated for 10 minutes at 100% amplitude with 10 seconds on and 1 second off. For the final 1mM working solution, 0.7mL of 50mM solution was added to cell growth media for a final volume of 35mL.

Untreated Controls: For each treatment, untreated controls contained only DMSO in the cell growth media. To match the treatments, 0.2 mL DMSO was added to 39.8 mL growth media for a final concentration of 0.5%. Final DMSO concentration were 0.4% for C1 and U1 and 0.125% for C2 and U2.

Treatments: Growth media was removed from each well and washed once with 1mL PBS. Treatments were then plated from the 1mM working solution to obtain 800uM

and 250uM solutions in the wells with the volumes made up to 1mL with cell growth media. Following treatment, plates were placed on a plate shaker at 150 rpm in an incubator at 37C and 5% CO_2.

Butyric acid: A 200mM solution, of Butyric acid (≥99%, Sigma Aldrich cat # B103500) was prepared in DMSO for a final volume of 1mL. To the pre-heated cell growth media, butyric acid stock solution (250uL) was added for a molarity of 50mM. The 50mM solution was sonicated for 10 minutes at 100% amplitude with 10 seconds on and 1 second off. For the final 1mM working solution, 0.7mL of 50mM solution was added to cell growth media for a final volume of 35mL.

3.2.4 Cell-based Assays

To ensure that the exposure to fatty acids over the time course did not induce significant cytotoxicity, apoptosis assays were carried out. The M30 Cytodeath Elisa (Peviva, Diapharma P10900) was used according to manufacturer's instructions. The ELISA contains the M30 antibody which specifically binds to keratin 18 after it has been cleaved by caspase (caspase cleaved keratin 18-CK18) as this occurs early in the apoptosis cycle (Leers et al., 1999). Keratin 18 is expressed in epithelial cells and is involved in the production of intermediate filaments of the cell cytoskeleton.

Cells were plated in 24-well plates and treated as stated above. Following treatment, cells were frozen at -80°C without removing treatment media. This would allow the cells to lyse and allow detection of all the CK18 in the treatment plates. Plates were allowed thaw at room temperature and 10% NP-40 (Thermofisher Cat. 28324) was

added for a final concentration of 0.5% (50uL in 1mL of Media) as per manufacturer's recommendation. NP-40 is a detergent which solubilizes the cell membranes including the nuclear membrane, allowing for measurement of all CK18 in the sample. Plates were shaken intermittently by hand for 5 minutes, pipetted up and down, and 25uL of sample was transferred to the M6 coated Microstrips. For the standards (zero/BLANK, low-250 U/L, medium-1000 U/L, and high-3000 U/L), 25uL of each was added to the plates in duplicates. Diluted M30 CytoDeath HRP conjugate (75uL) was added to each well and shaken at 600 rpm at room temperature for 4 hours. Wells were washed five time with wash solution and 200uL of TMB substrate was added to each well. Plates were incubated for 20 minutes in the dark. Following incubation, 50uL of stop solution was added to each well to terminate the reaction. The plate was immediately shaken for 5-10 seconds, and read at 450nm after 25 minutes on a BioTek ELx800 plate reader.

To determine if the fatty acid treatments result in increased amounts of lipid droplets, Oil Red O (ORO) assays were performed. ORO is a lipophilic dye that has an affinity for triglycerides and lipid droplets. After fixation, cells were stained with ORO and the excess dye was removed. For quantification, isopropanol was then used to extract the dye. The intensity of the extracted dye in isopropanol was detected with a plate reader. Increased storage of lipid droplets in hepatocytes would be indicative of dysregulated cell metabolism as hepatocytes do not store lipids.

Following treatment for the specified durations, cells were washed with 1mL PBS and fixed with 0.5mL 10% Neutral Buffered Formalin (Sigma Aldrich, cat # HT5011) was added to each well and incubated for 30 minutes to fix the cells. Wells were washed

twice with 1mL PBS. Oil Red O solution in glycol (0.5 mL) (Sigma Aldrich, cat # O1516) was added to each well and incubated for 30 minutes. Using a squirt bottle and ddH_2O, wells were carefully washed six times to remove excess Oil Red O from the wells. For imaging, 500uL of PBS was added to each well. Plates at this stage were kept at room temperature and covered until imaged. Drying of the wells would cause the cells to flatten and individual lipid droplets to fuse (macrovesicular lipid droplets) hindering visualization of microvesicular lipid droplets. Cells were imaged using an Olympus CKX41 Microscope with attached camera and the Cells Sense Entry software (Olympus) at a magnification of 40X For extraction of the stain from the fixed cells, isopropanol (750uL) was added to each well and incubated for 10 minutes on a plate shaker (150rpm). The isopropanol - oil red solution (200uL) was transferred to a 96-well plate and read at 490nm. A ratio was obtained by dividing the treated values by the untreated values. Statistical Analysis was conducted as a two-way ANOVA with Tukey post hoc testing using GraphPad Prism 7.03 (La Jolla, CA, USA).

3.2.5 DNA Extraction, Purification, and Quantification

Total DNA was extracted for ratio of mitochondrial to nuclear DNA quantification. For DNA extraction, following treatment, wells were washed twice with 2mL PBS. PBS (400uL) + Proteinase (40uL) (Qiagen, cat # 19131) was added to each well for cell lysis. The plates were swirled to ensure complete lysis. Buffer AL (400uL) (Qiagen, cat # 19075) was added to each well, swirled, and snap frozen at -80C. DNA was extracted using the Qiagen DNA Mini Blood Kit (Cat. 51104) as per manufacturer's

instructions. Plates were thawed at room temperature, and the well contents transferred to a 2mL centrifuge tube. Tubes were vortexed for 15sec and incubated at 56°C for 10min followed by brief centrifugation. To each tube, 400uL 100% ethanol was added and vortexed, followed by brief centrifugation. To a QIAmp Mini spin column in a 2mL collection tube, 600uL of the solution was added to a and spun at 8000rpm for 1 minute. The flow-through was discarded. These steps were repeated until all the cell solution had been passed through the column. With a new collection tube, but same column, 500uL buffer AW1 was added to each column, and spun at 8000rpm for 1 minute. The flow-through liquids were discarded, the columns placed in a new collection tube, and 500uL aliquots of buffer AW2 were added and spun at 13,200 rpm for 2 minutes. The flow-through liquids were discarded again, and the column placed in a new collection tube and spun at 13,200 rpm for 1 minute to remove any remaining buffer. A new collection tubes were used and 50uL of pre-warmed molecular grade H_2O (56°C) water aliquots were added directly to the filter in each column and incubated for 1 minute. Columns were spun at 8000rpm for 1 minute with the flow-through containing the DNA.

For spectrophotometric readings, 1uL of nucleic acid was diluted in 9uL of the elution solution and read using a Genequant 1300 (GE Healthcare, Cat # 28918215) with the units as ng/uL. To determine the purity of the sample, the 260/280 was determined with pure DNA having a ratio around 1.8 and pure RNA having a ratio around 2.0. To determine if chemical contamination was present due to carryover from the washes, the 260/230 ratio measured with a standard range being 2 – 2.2.

Mitochondrial DNA (mtDNA) copy number is a critical determinant of overall mitochondrial health. Through a quantitative, real-time PCR reaction, relative mtDNA content was determined through amplification of a single gene from both the mitochondrial and nuclear genomes. Relative mtDNA quantity was determined by comparing it to diploid nuclear DNA amount (HVS/B2M assay). As the number of mitochondria, and thus the amount of mitochondrial DNA, can fluctuate between cell and tissue types, standardization to nuclear DNA allowed for quantification as total nuclear DNA does not fluctuate. Primers used were targeted to regions present in a single copy number.

For determination of ratio of mitochondrial to nuclear DNA, two genomic regions were targeted: 1) B2M, a single-copy nuclear locus, and 2) a mitochondrial DNA site in the minor arc, which is on the heavy strand and includes the origin of replication, where large deletions are rare (mtMinArc) (Phillips et al., 2014). *B2M* (GenBank accession number: NG 012920) has been previously reported to be present in single copy number (Malik et al., 2011).

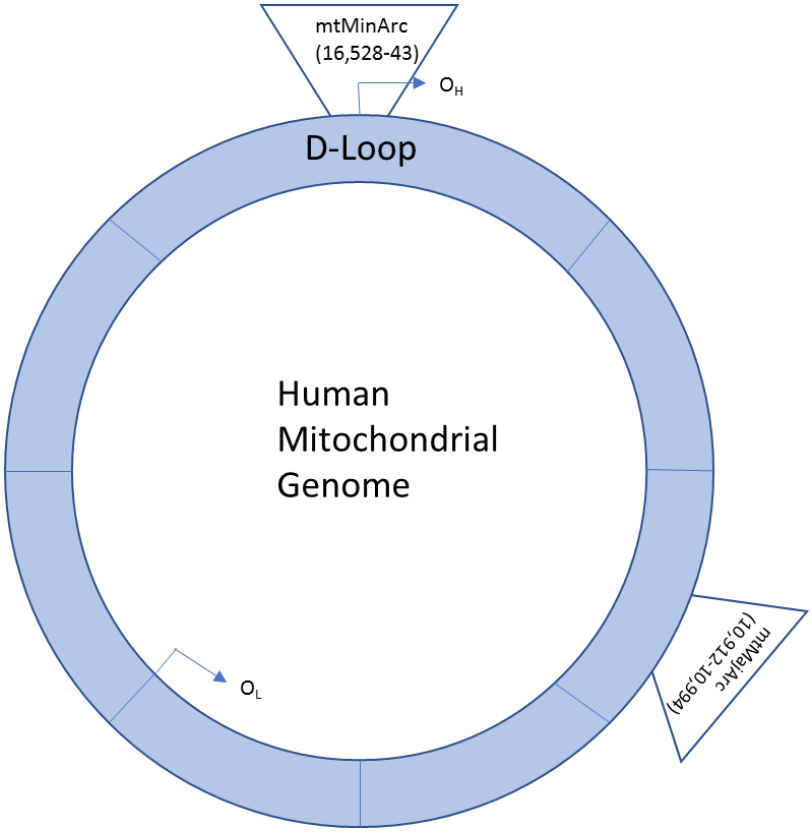

Figure 4: Location of MinArc and MajArc in the human mitochondrial genome (Adapted from (Phillips et al., 2014)

For intra- and inter-plate control, control DNA was used with a HVS3 primer. Samples were run in duplicate with a final concentration of 1ng/uL of DNA in a 10uL reaction volume and a final primer concentration of 250uM. No template controls were run for each primer on every run.

The protocol initiated with denaturation at 98°C for 30 seconds. 40 cycles followed with each cycle consisting of 1) denaturation at 95°C for 30 seconds, 2) annealing at 60°C for 1 minute, 3) annealing at 72°C for 1 minute, and 4) extension and

collection of amplification data. A dissociation curve followed and consisted of incubation 65°C for 5 sec, and a ramp up to 95°C. Melt-curves were used to ensure specificity. MtDNA copy number, relative to nuclear DNA, was determined using the $2^{-\Delta Ct}$ method. Treated Ct values were obtained by subtracting the mitochondrial Ct value from the nuclear Ct value to obtain a $\Delta Ct_{Treated}$ value, with the same procedure done for the untreated values. $\Delta Ct_{Treated}$ and $\Delta Ct_{Untreated}$ values were log transformed and provided a value for the relative ratio of mitochondrial to nuclear DNA. Statistical Analysis was conducted as a two-way ANOVA with Tukey post hoc testing using GraphPad Prism 7.03 (La Jolla, CA, USA).

Table 1: Primer Sequences

Assay	Primer Name	Sequence	Product Length
Ratio of mitochondrial to nuclear DNA	Mito DNA	F-5`ACATAGGGTGCTCCGGCT R-5`ACAAGCAAGTACAGCAATCAACC	489bp
	Nuclear *B2M*	F-5' GCTGGGTAGCTCTAAACAATGTATTCA R-5' CATGTACTAACAAATGTCTAAAATGGT	95bp
Gene expression	*ACTB*	F-5' CTCTTCCAGCCTTCCTTCCT R-5' AGCACTGTGTTGGCGTACAG	116bp
	ACOX1	F-5' CCTTGCTTCACCAGGCAACTG R-5' ATGATTTGAAGTCTTTCCAAGCCCA	230bp
	ACADM	F-5' TGGAAGCAGATACCCCAGGA R-5' CAGCACCAGCAGCTACTACA	195bp
	CPT-1a	F-5' TTTGGACCGGTTGCTGATGA R-5' TTTCCAGCCCAGCACATGAA	222bp
	MFn2	F-5' GAAGGTGAAGCGCAATGTCC R-5' CTTCTGTGGTAACGGGGTCC	231bp
	PPARGC 1A	F-5' AGTGACATCGAGTGTGCTG R-5' AGTGTCTCTGTGAGGACTGC	245bp
	TFAM	F-5' CGCTCCCCCTTCAGTTTTGT R-5' CCAACGCTGGGCAATTCTTC	177bp

3.2.6 RNA Extraction

For RNA extractions, following treatment, wells were washed twice with 2mL PBS, and the plates were snap frozen at -80C with no liquid in the wells. RNA was extracted using the Biorad Aurum Total RNA Mini Kit (Cat. 7326820). Wells were removed from the freezer and 1mL of PureZOL (Cat. 7326890) was immediately added to each well and allowed to come to room temperature. Once at room temperature, the wells were incubated for 15 minutes and the solution transferred to 2mL centrifuge tubes. 200uL of chloroform was added to each tube and shaken for 15 seconds. Tubes were incubated at room temperature for 5 minutes with shaking every minute. Tubes were centrifuged at 12,000 rpm for 15 minutes at 4˚C. The aqueous phase was removed and transferred to a new 2mL tube. A volume of 70% ethanol equal to the volume of the removed aqueous phase was added to each tube and mixed by pipetting. The ethanol + aqueous phase mixture (700uL) of the mixture was added to a RNA binding column and spun at >12,000 rpm for 1 minute with the flow-through discarded. This was repeated with the remaining sample. Low stringency wash solution (700uL) was added to each tube and spun at 12,000 rpm for 30 seconds with the flow-through discarded. This step was repeated with the high stringency wash solution followed by the low stringency wash solution. Columns were transferred to 2mL centrifuge tubes and 30uL of pre-warmed molecular H_2O was added directly to the filter of each column and incubated for 1 minute. Columns were centrifuged at >12,000 rpm for 2 minutes with the flow-through containing the RNA. The tubes were immediately placed on ice. For spectrophotometry

readings, 1uL of RNA was diluted in 9uL of the same water used for elution and read using a Genequant 1300 machine with the units as ng/uL.

3.2.8 cDNA Synthesis

To determine the relative expression of genes involved in mitochondrial homeostasis and lipid processing, cDNA was made from the extracted RNA. As the primers chosen, listed below, are designed for mRNA, the cDNA concentration must be high enough to measure mRNA as it only constitutes around 1%-5% of extracted total RNA. For cDNA synthesis, the BioRad iScript cDNA synthesis kit (Biorad, #1708890) was used. For each sample of extracted RNA, the concentration was divided by 1000 to determine to volume needed for 1ug/uL of cDNA. This volume was made up to 15uL with nuclease-free water. For each sample, 4uL of 5x iScript reaction mix, 1uL of iScript reverse transcriptase, and 15uL of RNA template and water were added to a microcentrifuge tube, with the total volume being 20uL. In a thermocycler, the protocol followed was priming for 5 minutes at 25˚C, reverse transcription for 20 minutes at 46˚C, inactivation for 1 minute at 95˚C, and holding at 4˚C. The samples were then transferred to 4˚C until ready to use.

3.2.9 Evaluation of Mitochondrial Homeostasis and Lipid Processing Genes by qPCR

Quantitative real-time PCR was performed in a 96-well format on a Biorad CFX96 Real Time System (BioRad Laboratories, USA). Reaction mixtures, in a total volume of 10uL, consisted of 1uL cDNA (1ug of total RNA), 0.25uM Real-Time primers, and 1x SsoFast Evagreen Supermix (Biorad, USA). No template controls were

used to detect for contamination. The protocol initiated with denaturation at 95°C for 30 seconds. 40 cycles followed with each cycle consisting of 1) denaturation at 95°C for 10 seconds, 2) annealing at 60°C for 40 seconds, and 3) extension and collection of amplification data. A dissociation curve followed and consisted of incubation 65°C for 5 seconds, and a ramp up to 95°C. Melt-curves were used to ensure specificity.

Ct values were standardized to ACTB and the expression ratio of the treated samples was calculated by normalization to the untreated controls with the ΔΔCt method. Statistical Analysis was conducted as a two-way ANOVA with Tukey post hoc testing using GraphPad Prism 7.03 (La Jolla, CA, USA).

CHAPTER FOUR: RESULTS

4.1 Study Design

Following treatment of cells with one or another lipid variety, this study proceeded with two sets of experiments (Figure 4). In the first set, cells were stained with Oil Red O to measure intracellular lipid accumulation. In the second set, both types of nucleic acids, DNA and RNA, were extracted. DNA was used for ratio of mitochondrial to nuclear DNA. RNA was converted to cDNA and was used as the template to measure expression of genes involved in mitochondrial and lipid homeostasis. Additionally, we investigated the hypothesis that the treatments with fatty acids may directly lead to cellular apoptosis.

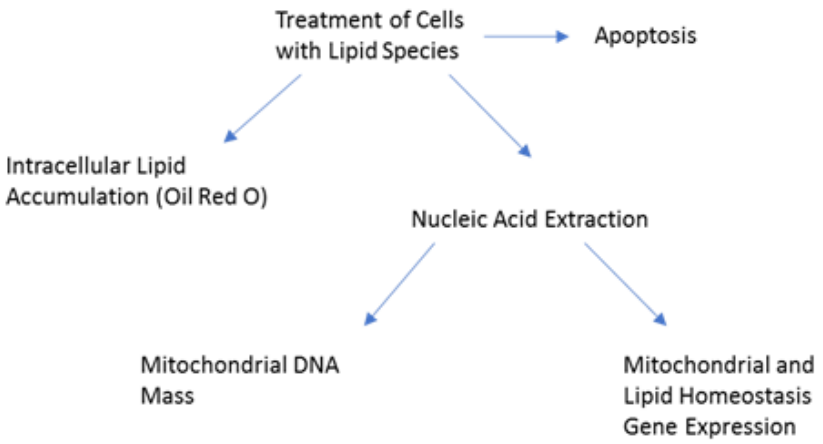

Figure 5: Study Design

4.2 A study of Lipid Accumulation in HepG2 cells Exposed to Oleic, Palmitic, or Butyric acids

The pathophysiology of NAFLD and NASH has many links with hepatic lipid metabolism. The first hit is excessive hepatic fat accumulation. Therefore, in our study, HepG2 cells were treated with three different lipid species: Oleic, Palmitic, and Butyric Acid to mimic the influx of excess FFAs into hepatocytes.

4.2.1 Time Course of Lipid Accumulation in Response to the Treatment with Palmitic, Oleic or Butyric Acids

To understand changes in lipid accumulation in response to a) exposure to different lipid species, b) different lipid concentrations, and c) exposure duration, Oil Red O assays were carried out. This dye stains intracellular lipids, enabling their quantification. For this assay, Oil Red dye extracted from HepG2 cells exposed to lipids and the untreated control cells was quantified at an absorbance of 490nm.

Exposure to Oleic Acid Does Not Influence Lipid Accumulation:

In HepG2 hepatocytes exposed to oleic acid, lipid accumulation was not significantly altered over time (2-24 hrs) ($p=0.58$) (Table 2 and Figure 6) or in response to a final media concentration of 800uM or 250uM.

Table 2: The Results of Oleic Acid Lipid Accumulation Assay

Oleic acid Normalized Fold-Change	Sum of Squares	Degrees of Freedom	Mean Squares	F (DFn, Dfd)	P-Value
Interaction	0.04437	4	0.01109	F (4, 20) = 0.8004	P=0.5391
Time	0.04064	4	0.01016	F (4, 20) = 0.7331	P=0.5801
Normalized Concentration (800uM vs. 250uM)	0.0001415	1	0.0001415	F (1, 20) = 0.01021	P=0.9205

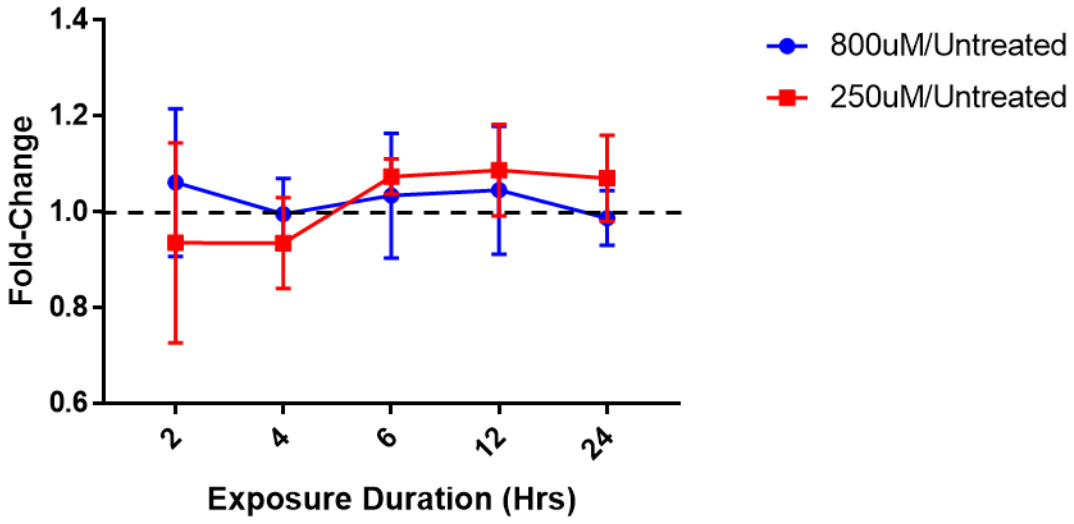

Figure 6: The Results of an Assay for Oleic Acid Induced Lipid Accumulation. This assay quantified the effects of exposure to oleic acid at a final media concentration of 800uM and 250uM on lipid accumulation in HepG2 cells. Fold changes reflect the ratio of the lipid contents in oleic acid treated cells to that in control cells (untreated).

Exposure to Palmitic Acid Results in Altered Lipid Accumulation:

Lipid accumulation in cells treated with palmitic acid was altered significantly over exposure time (p=0.049) in response to a final media concentration of 800uM palmitic acid, but not in response to 250uM palmitic acid (Table 3 and Figure 7). Post Hoc comparison, aimed at identifying the time points where lipid accumulation rates differed most significantly, revealed maximum lipid accumulation at 6 hours, while a significant decrease was observed at 24 hours following treatment with a final media concentration of 800uM palmitic acid (MD=0.3084, p=0.0185) (Figure 7).

Table 3: The Results of an Assay of Palmitic Acid Dependent Lipid Accumulation. Significant values are in bold.

Palmitic Acid Normalized Fold-Change	Sum of Squares	Degrees of Freedom	Mean Squares	F (DFn, Dfd)	P-Value
Interaction	0.09334	4	0.02333	F (4, 20) = 1.962	P=0.1394
Time	0.1373	4	0.03431	F (4, 20) = 2.885	**P=0.0490**
Normalized Concentration (800uM vs. 250uM)	0.01102	1	0.01102	F (1, 20) = 0.9265	P=0.3473

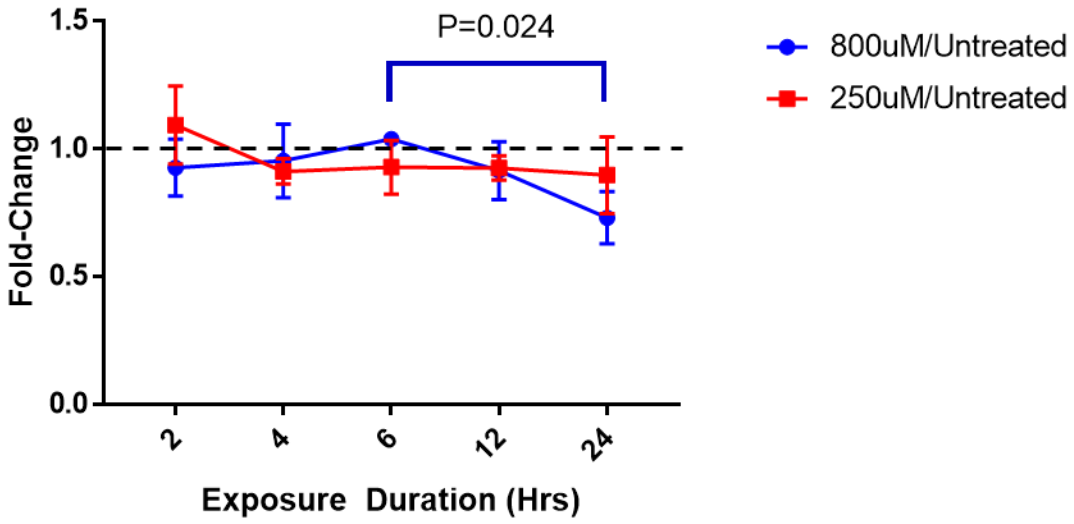

Figure 7: The Results of an Assay of Palmitic Acid Induced Accumulation of Lipid. This assay quantified the effects of exposure to a final media concentration of palmitic acid at 800uM and 250uM on lipid accumulation in HepG2 cells. Fold changes reflect the ratio of the lipid contents in treated cells to that in control cells (untreated).

Both Duration of Exposure and Concentration of Butyric Acid Alter Lipid Accumulation:

In cells treated with butyric acid, lipid accumulation was significantly affected by both treatment duration ($p=0.0005$) and concentration ($p=0.0009$) (Table 4 and Figure 8). ANOVA testing showed the interaction between these two factors to be significant and positive ($F=4.7$; $p=0.008$), suggesting that accumulation of lipid increases with an increase in exposure time as well as concentration. Post hoc testing for time course experiment with 800uM butyric acid (Table 4) showed that significant and maximum lipid accumulation was observed at 24 hours (FC=1.59) compared to other time points, while treatment with a lower butyric acid concentration (250uM) showed maximum lipid accumulation to occur significantly within the first 2 hours (FC = 0.99), followed by a decrease in intracellular lipid accumulation noticeable at 12 hours (FC=0.87) (Table 5).

Table 4: The Results of an Assay for Butyric Acid Dependent Lipid Accumulation. Significant values are highlighted in bold.

Butyric Acid Normalized Fold-Change	Sum of Squares	Degrees of Freedom	Mean Squares	F (DFn, Dfd)	P-Value
Interaction	0.331	4	0.08275	F (4, 20) = **4.683**	**P=0.0079**
Time	0.562	4	0.1405	F (4, 20) = 7.951	**P=0.0005**
Normalized Concentration (800uM vs. 250uM)	0.2649	1	0.2649	F (1, 20) = 14.99	**P=0.0009**

Table 5: The Fold Changes in Lipid Accumulation Following the Treatment with Butyric Acid. Significantly different values are shown in bold.

Time	Normalized 800uM Fold Change	Normalized 250uM Fold Change
2 Hrs	1.111391	**1.003645**
4 Hrs	0.953179	0.932453
6 Hrs	1.106254	0.942436
12 Hrs	0.922054	0.871132
24 Hrs	**1.589516**	0.993015

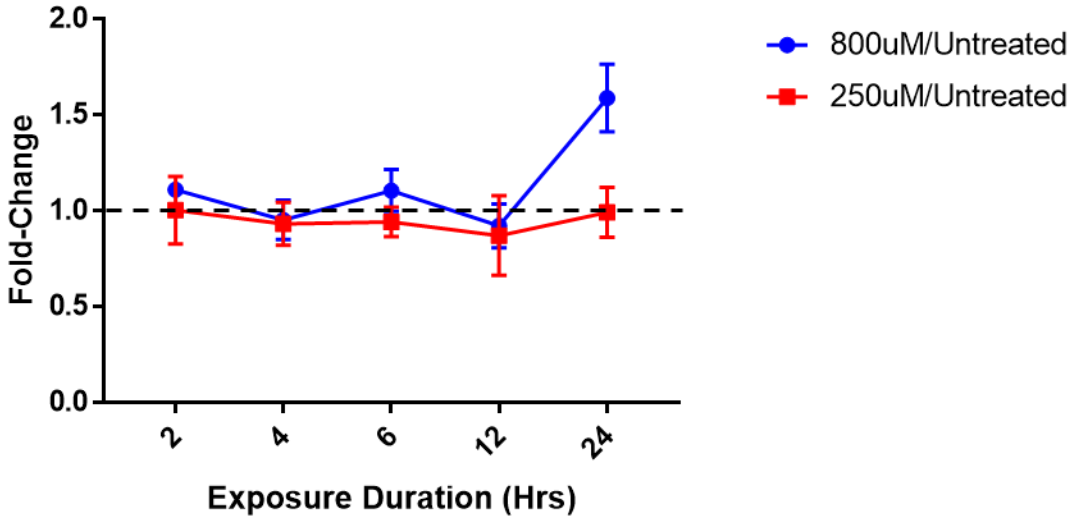

Figure 8: The Results of Butyric Acid-induced Lipid Accumulation Assay. This Assay quantified the effects of exposure to butyric acid at a final concentration of 800uM and 250uM in the media on lipid accumulation in HepG2 cells. Fold change values reflect the ratio of the lipid contents in butyric acid treated cells to that in control cells (untreated).

4.2.2 Lipid Accumulation is Altered in HepG2 Cells Exposed to Either 800uM or 250uM Butyric Acid

To explore the effect of dose response, data was analyzed independently for the three lipid species. At a final media concentration of 800uM and 250uM, no significant change in lipid accumulation was seen when HepG2 cells were exposed to oleic acid ($p=0.92$, Table 2) or palmitic acid ($p=0.347$, Table 3). In cells treated with butyric acid, however, lipid accumulation was significantly altered in response to a change in concentration ($p=0.0009$, Table 4). This change in lipid accumulation was also dependent on time as indicated by a significant interaction score in ANOVA testing ($p=0.0079$). In presence of 800uM butyric acid, maximum lipid accumulation was observed at 24 hours

(FC=1.59), while in presence of a final media concentration of 250uM butyric acid, no change in lipid accumulation was observed at 2 hours (FC=1, Table 5).

4.3 A Study of Changes in the Ratio of Mitochondrial to Nuclear DNA in HepG2 cells Exposed to Palmitic, Oleic or Butyric Acids

To understand changes in the ratio of mitochondrial to nuclear DNA in response to lipid species, lipid concentration, and duration exposure, qPCR was carried out to measure the levels of mitochondrial DNA relative to nuclear DNA using mitochondrial and nuclear specific primers. Results were expressed as a ratio of the copy number of mitochondrial DNA to nuclear DNA.

4.3.1 Time Course Changes in the Ratio of Mitochondrial to Nuclear DNA in Response to the Treatment with Palmitic, Oleic or Butyric Acids

Oleic Acid:

To explore the effect of oleic acid on the ratio of mitochondrial to nuclear DNA of HepG2 cells, ANOVA tests were performed. A positive and significant interaction between the exposure duration and concentration ($F=2.11$, $p=0.0424$, Table 6) was shown. However, neither time of exposure nor concentration alone had significant effect on the ratio of mitochondrial to nuclear DNA.

Table 6: The Effects of Exposure to Oleic acid on the Ratio of Mitochondrial to Nuclear DNA Significant values are in bold.

Ratio of Mitochondrial to Nuclear DNA – Oleic acid	Sum of Squares	Degrees of Freedom	Mean Squares	F (DFn, Dfd)	P-Value
Interaction	3.236	4	0.8089	F (4, 20) = 3.017	**P=0.0424**
Time	2.713	4	0.6782	F (4, 20) = 2.53	P=0.0727
Normalized Concentration (800uM vs. 250uM)	0.0003391	1	0.0003391	F (1, 20) = 0.001265	P=0.9720

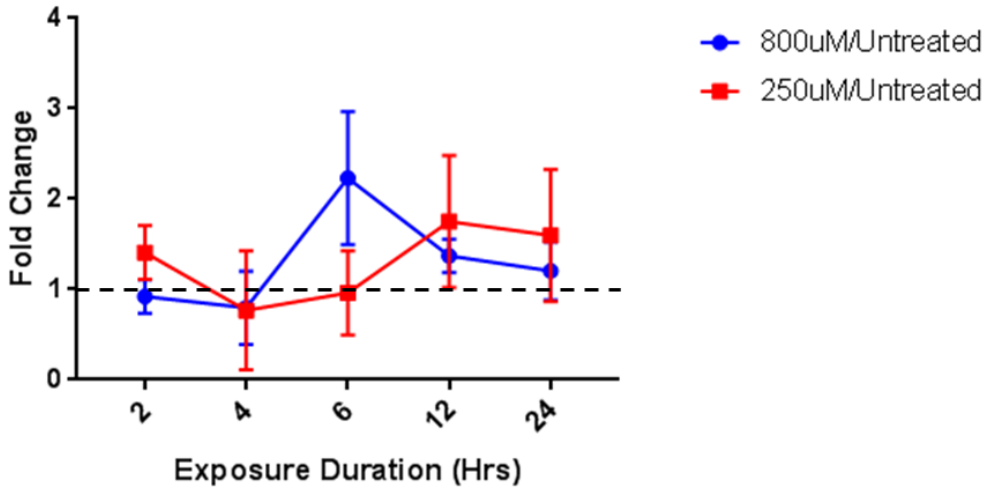

Figure 9: The Effects of Exposure to Oleic Acid on the Ratio of Mitochondrial to Nuclear DNA. The Results of the oleic acid ratio of mitochondrial to nuclear DNA Assay, which quantified the effects of oleic acid at a final media concentration of 800uM or 250uM on the ratio of mitochondrial to nuclear DNA. Fold changes reflect the ratio of ratio of mitochondrial to nuclear DNA in oleic acid treated cells to that in control cells (untreated).

Palmitic Acid:

In cells treated with palmitic acid, the ratio of mitochondrial to nuclear DNA was significantly altered by both treatment duration and concentration as indicated by a positive and significant interaction between these parameters (F=3.168, p=0.0361) (Table 7). Further, time alone had a positive and significant effect on the change in the ratio of mitochondrial to nuclear DNA (F=4.0, p=0.014), while concentration did not have a significant effect. Additional post hoc comparison revealed that the treatment of cells with a concentration 800uM of palmitic acid in the media lead to an increase in the ratio of mitochondrial to nuclear DNA after 4 hours post-exposure as compared to 24 hours (MD=0.87, p=0.0296, Figure 10).

Table 7: The Effects of the Exposure to Palmitic Acid on the Ratio of Mitochondrial to Nuclear DNA. Significant values are in bold.

Ratio of Mitochondrial to Nuclear DNA – Palmitic acid	**Sum of Squares**	**Degrees of Freedom**	**Mean Squares**	**F (DFn, Dfd)**	**P-Value**
Interaction	1.377	4	0.3443	F (4, 20) = 3.168	**P=0.0361**
Time	1.753	4	0.4382	F (4, 20) = 4.032	**P=0.0148**
Normalized Concentration (800uM vs. 250uM)	0.3357	1	0.3357	F (1, 20) = 3.089	P=0.0941

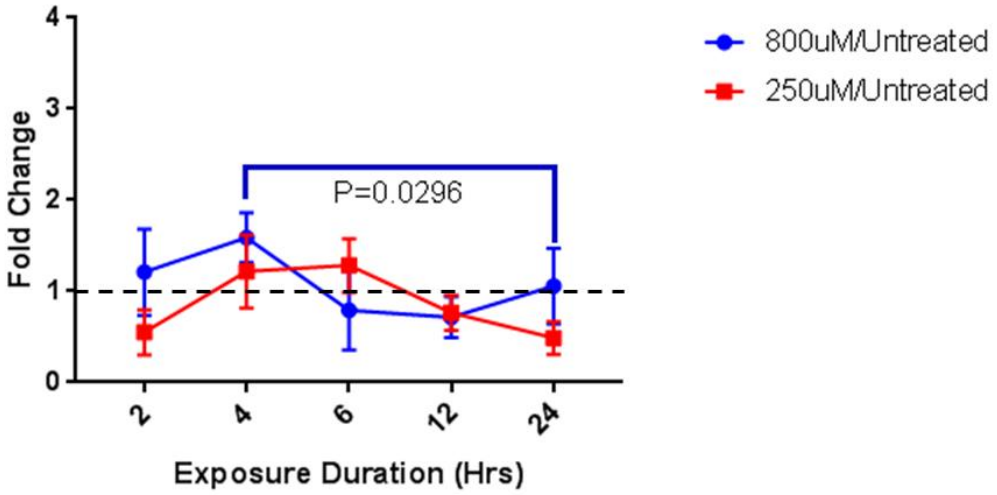

Figure 10: The Effects of Exposure to Palmitic Acid on the Ratio of Mitochondrial to Nuclear DNA. The results of the palmitic acid ratio of mitochondrial to nuclear DNA Assay, which quantified the effects of palmitic acid at a media concentration of 800uM or 250uM on the ratio of mitochondrial to nuclear DNA. Fold changes reflect the ratio of ratio of mitochondrial to nuclear DNA in palmitic acid treated cells to that in control cells (untreated).

Butyric Acid:

Exposure to either a concentration of 800uM or 250uM of butyric acid in the media had no significant effect on ratio of mitochondrial to nuclear DNA over time (2-24hrs) (Table 8).

Table 8: The Effects of the Exposure to Butyric Acid on the Ratio of Mitochondrial to Nuclear DNA. Significant values are in bold.

Ratio of Mitochondrial to Nuclear DNA – Butyric acid	Sum of Squares	Degrees of Freedom	Mean Squares	F (DFn, Dfd)	P-Value
Interaction	0.9104	4	0.2276	F (4, 20) = 2.114	P=0.1168
Time	0.3013	4	0.07531	F (4, 20) = 0.6997	P=0.6012
Normalized Concentration (800uM vs. 250uM)	0.2701	1	0.2701	F (1, 20) = 2.51	P=0.1288

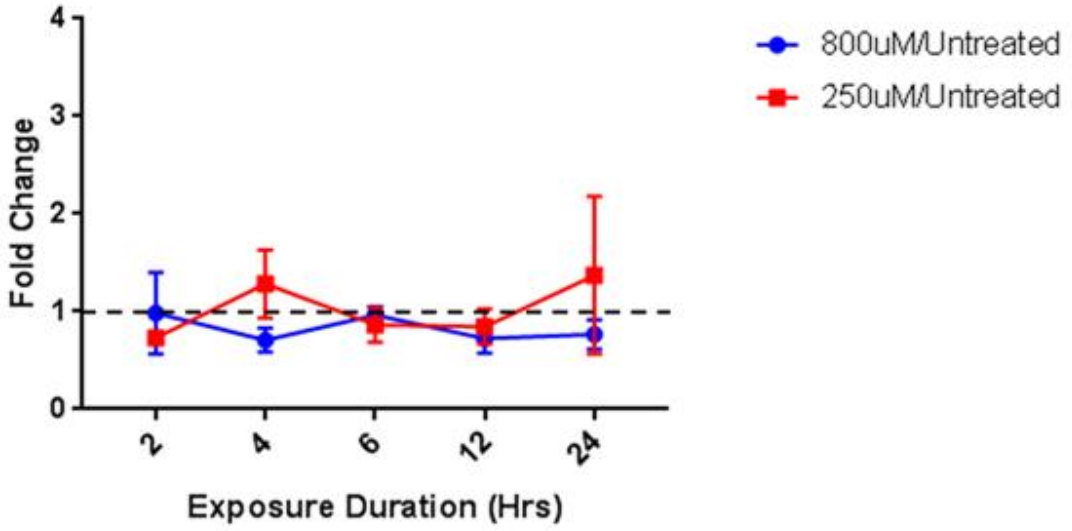

Figure 11: The Effects of Exposure to Butyric Acid on the Ratio of Mitochondrial to Nuclear DNA. The results of the butyric acid ratio of mitochondrial to nuclear DNA Assay, which quantified the effects of butyric acid at a media concentration of 800uM or 250uM on the ratio of mitochondrial to nuclear DNA. Fold changes reflect the ratio of ratio of mitochondrial to nuclear DNA in butyric acid treated cells to that in control cells (untreated).

4.3.2 Changes in Lipid Concentration Resulted in No Changes in the Ratio of Mitochondrial to Nuclear DNA Following Exposure to Oleic, Palmitic, or Butyric Acid

To explore the effects of concentration on the ratio of mitochondrial to nuclear DNA changes, the ratio of mitochondrial to nuclear DNA was measured following

independent exposure to 2 concentrations (800uM and 250uM in the final media) of the three independent lipids. The ratio of mitochondrial to nuclear DNA was not significantly altered with 800uM or 250uM of oleic acid (p=0.97, Table 6, Figure 9). Similar results were seen in cells treated with 800uM or 250uM palmitic acid (p=0.094, Table 7, Figure 10), and butyric acid (p=0.129, Table 8, Figure 11 respectively). This suggests lipid treatment alone has no effect on the ratio of mitochondrial to nuclear DNA.

4.4 Apoptosis

To ensure that changes seen in lipid accumulation, the ratio of mitochondrial to nuclear DNA, and gene expression were not due to a difference in the number of cells. An ELISA for apoptosis was conducted.

The apoptosis assay was carried out with an R^2 value of 1 for the standard curve, however all samples, except those treated with palmitic acid in a final media concentration of 800uM for 24 hours, were below the level of detection at 450nm. Exposure to palmitic acid in a final media concentration of 800uM for 24 hours resulted in significant detectable levels of CK18 (mean= 1463.7, SD=735.19).

4.6 Changes in the Levels of mRNAs Encoding Genes Involved in Mitochondrial Homeostasis and Lipid Processing

To understand changes in expression in genes involved in mitochondrial homeostasis and lipid processing in response to lipid species, lipid concentration, and exposure duration, qPCR experiments were conducted. Resultant data was analyzed after normalization of expression values to that of the reference gene (ACTB). Fold changes in

mRNA levels were obtained by a ratio of treated mRNA levels to mRNA levels of untreated controls. Assays were run in duplicate.

4.6.1 Effects of Oleic acid on Expression of Various Genes Involved in Lipid Metabolism and Mitochondrial Homeostasis

4.6.1.1 *CPT-1a* mRNA Levels Were Altered in Response to Changes in Oleic Acid Concentration, but not to Time

In HepG2 hepatocytes exposed to oleic acid, *CPT-1a* mRNA levels were not significantly altered over time (2-24 hours) (p=0.1242), but were significantly altered in response to concentration (800uM or 250uM in the media) (p=0.0053, Table 9, Figure 12). As only two replicates were obtained per time point, statistical comparison of mRNA levels of treated to untreated control cells was not possible. Therefore, we calculated a fold change values to use in our comparison. Following exposure to 800uM, the fold change of *CPT-1a* mRNA levels was decreased at 4, 6, 12 and 24 hours post exposure (FC=0.79, FC=0.40, FC=0.22, FC=0.21 respectively) compared to non-exposed HepG2 controls across all time points. However, following exposure to 250uM, the fold change in *CPT-1a* mRNA levels displayed a fluctuating pattern between 2-12 hours, followed by a decrease as compared to untreated control HepG2 cells at 24 hours (FC=0.57, Table 10).

Table 9: The Changes in *CPT-1a* mRNA Levels Following Oleic Acid Treatment. Significant values are in bold.

***CPT-1a* mRNA Levels**	**Sum of Squares**	**Degrees of Freedom**	**Mean Squares**	**F (DFn, Dfd)**	**P-Value**
Interaction	1.147	4	0.2867	F (4, 10) = 1.693	P=0.2274
Time	1.594	4	0.3984	F (4, 10) = 2.354	P=0.1242
Normalized Concentration (800uM vs. 250uM)	2.126	1	2.126	F (1, 10) = 12.56	**P=0.0053**

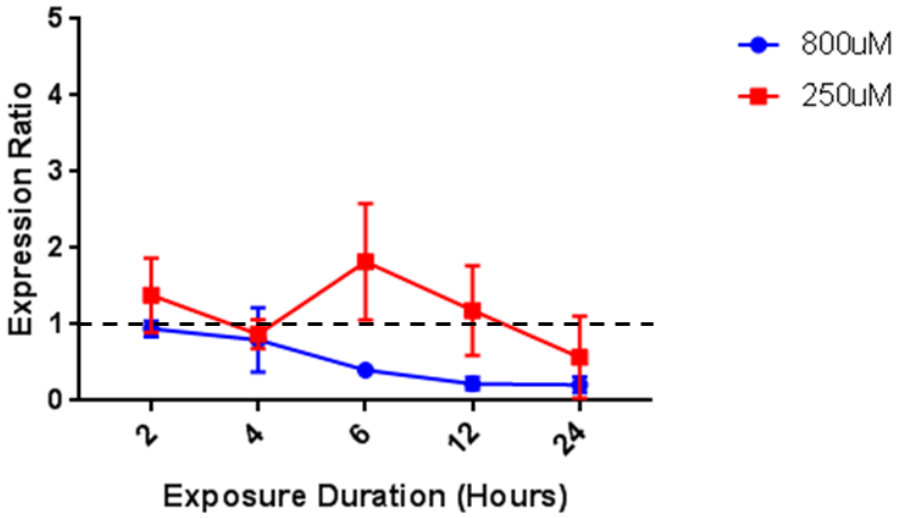

Figure 12: The Changes in *CPT-1a* mRNA Levels Following Oleic Acid Treatment. This assay quantified the effects of exposure to oleic acid at a final media concentration of 800uM and 250uM on *CPT-1a* mRNA levels. The expression ratio reflects the ratio of the expression in oleic acid treated cells to that in control cells (untreated).

Table 10: Fold Change (Treated/Untreated) in mRNA Levels Following Exposure to Oleic Acid

	800uM Fold Change	250uM Fold Change
CPT-1a		
2 Hrs	0.942255	1.383849
4 Hrs	0.797147	0.873827
6 Hrs	0.400868	1.821172
12 Hrs	0.224253	1.186015
24 Hrs	0.210004	0.570269
ACADM		
	Fold Change	Fold Change
2 Hrs	1.526846	1.192865
4 Hrs	1.655547	0.688965
6 Hrs	0.961131	1.121946
12 Hrs	0.789828	2.007405
24 Hrs	0.825093	0.905201
ACOX1		
2 Hrs	0.828831	0.700876
4 Hrs	1.027888	0.78533
6 Hrs	0.964607	1.063499
12 Hrs	0.883736	1.494993
24 Hrs	0.744831	1.223313
MFn2		
2 Hrs	0.562579	2.527291
4 Hrs	0.769628	1.695512
6 Hrs	1.24205	1.113373
12 Hrs	0.669847	1.085493
24 Hrs	1.339061	0.596652
PPARGC1A		
2 Hrs	1.017737	1.276259
4 Hrs	1.06713	1.639451
6 Hrs	1.12961	0.915536
12 Hrs	0.188895	1.269199
24 Hrs	0.922928	0.448766

TFAM		
2 Hrs	0.538687	1.253351
4 Hrs	0.496198	0.796957
6 Hrs	0.297874	1.250766
12 Hrs	0.213803	1.086907
24 Hrs	0.143163	0.80878

4.6.1.2 *TFAM* mRNA Levels were Altered in Response to Varying Concentrations of Oleic Acid

Mitochondrial Transcription Factor A (*TFAM)* mRNA levels were not significantly altered in response to exposure duration (2-24 hrs) (p=0.4846), however concentration (800uM or 250uM in the media) significantly altered expression (p=0.0007, Table 11, Figure 13). Following exposure to oleic acid at a final media concentration of 800uM, *TFAM* mRNA levels were decreased compared to untreated controls across all time points. However, following exposure to oleic acid at a final media concentration of 250uM, *TFAM* mRNA levels displayed a cyclical pattern between 2-12 hours, followed by a decrease compared to untreated controls at 24 hours (FC=0.81) (Table 10).

Table 11: The Changes in TFAM mRNA Levels Following Oleic Acid Treatment

TFAM mRNA Levels	**Sum of Squares**	**Degrees of Freedom**	**Mean Squares**	**F (DFn, Dfd)**	**P-Value**
Interaction	0.2547	4	0.06367	F (4, 10) = 0.5992	P=0.6717
Time	0.3952	4	0.09881	F (4, 10) = 0.9298	P=0.4846
Normalized Concentration (800uM vs. 250uM)	2.46	1	2.46	F (1, 10) = 23.15	**P=0.0007**

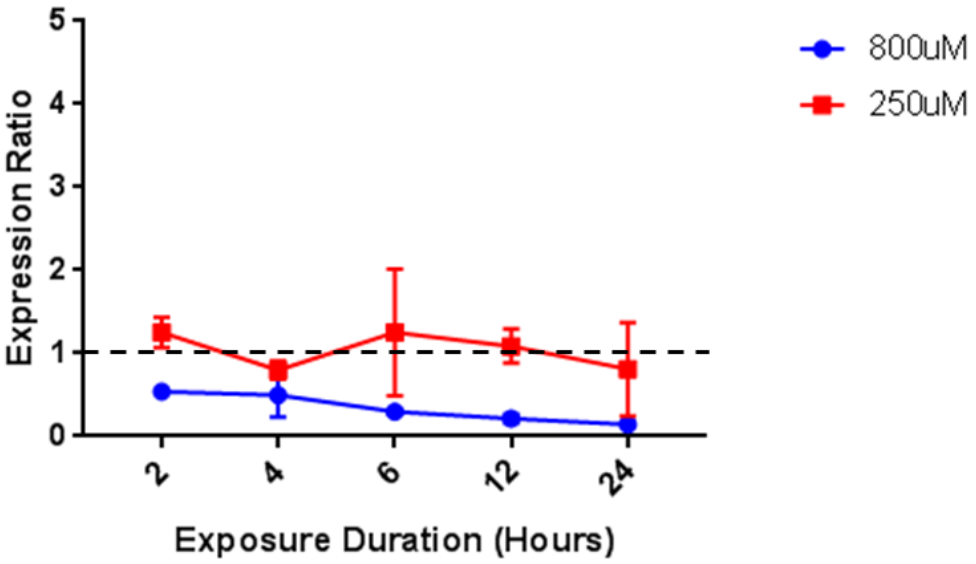

Figure 13: The Changes in *TFAM* mRNA Levels Following Oleic Acid Treatment. This assay quantified the effects of exposure to oleic acid at a final media concentration of 800uM and 250uM on mRNA levels of *TFAM*. The expression ratio reflects the ratio of the expression in oleic acid treated cells to that in control cells (untreated).

4.6.1.3 Exposure to Oleic Acid Significantly Alters *CPT-1a* and *TFAM* mRNA Levels

In cells treated with oleic acid, prolonging exposure had no effect on expression of *CPT-1a* and *TFAM* mRNA. However, expression levels for these genes were significantly different between cells treated with 800uM and with 250uM oleic acid, p =0.0053 for *CPT-1a* (Table 9) and p=0.0007 (Table 11), respectively. Levels of mRNAs transcribed from *ACADM* (p=0.8879), *ACOX1* (p=0.1952), *MFn2* (p=0.1197), and *PPARGC1A* (p=0.1342) did not differ significantly following treatment with either 800uM or 250uM oleic acid or changes in exposure duration.

4.6.2 Effects of Palmitic Acid on Expression of Various Genes Involved in Lipid Metabolism and Mitochondrial Homeostasis

4.6.2.1 Exposure to Palmitic Acid Alters *CPT-1a* mRNA Levels

CPT-1a mRNA levels were not significantly altered in response to exposure duration (2-24 hrs) (p=0.1832), but were significantly altered in response to concentration (800uM or 250uM) (p=0.0133) (p=0.1832) (Table 12). As only two replicates were obtained per time point, statistical comparison of mRNA levels of treated to untreated control cells was not possible due to this, we calculated a fold change value to use in our comparison. Following exposure to 800uM palmitic acid, the fold change (FC) in *CPT-1a* mRNA levels was higher than those in untreated control cells from at 2 hours post exposure (FC=1.42) and from 6-24 hours (FC=3.51, FC=3.58, FC= 4.7 respectively) (Table 13). Exposure to 250uM palmitic acid resulted in a similar increase from 6-12 hours (FC=1.74, FC=1.68 respectively), followed by a decrease in the fold change of *CPT-1a* mRNA levels at 24 hours compared to untreated control cells (FC=0.64) (Table 10).

Table 12: The Changes in *CPT-1a* mRNA Levels Following Palmitic Acid Treatment. Significant values are in bold.

CPT-1a mRNA Levels	**Sum of Squares**	**Degrees of Freedom**	**Mean Squares**	**F (DFn, Dfd)**	**P-Value**
Interaction	9.065	4	2.266	F (4, 10) = 1.4	P=0.3024
Time	12.44	4	3.111	F (4, 10) = 1.922	P=0.1832
Normalized Concentration (800uM vs. 250uM)	14.58	1	14.58	F (1, 10) = 9.012	**P=0.0133**

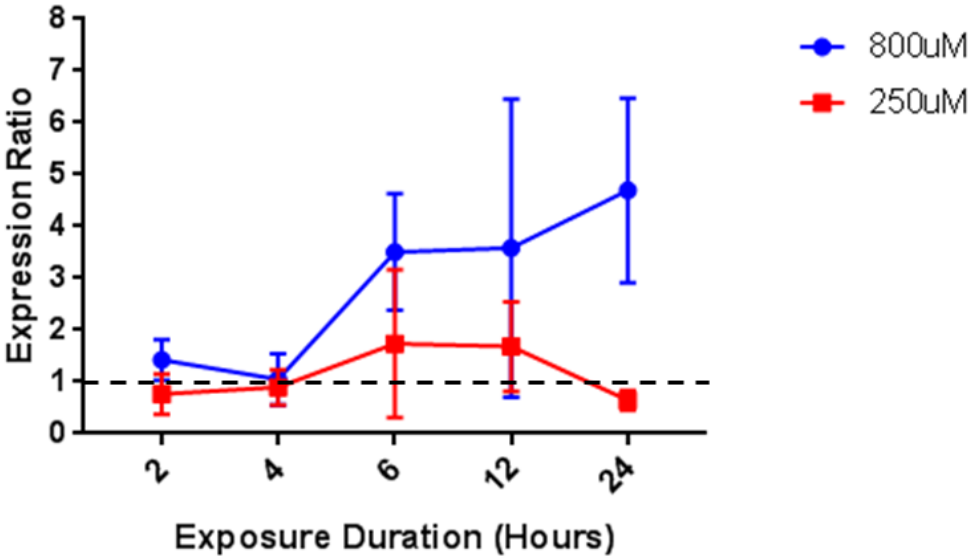

Figure 14: The Changes in *CPT-1a* mRNA Levels Following Palmitic Acid Treatment. This assay quantified the effects of exposure to palmitic acid at a final media concentration of 800uM and 250uM on *CPT-1a* mRNA levels. The expression ratio reflects the ratio of the expression in palmitic acid treated cells to that in control cells (untreated).

Table 13: Fold Change (Treated/Untreated) of mRNA Levels Following Exposure to Palmitic Acid

	800uM Fold Change	250uM Fold Change
CPT-1a		
2 Hrs	1.424558	0.76174
4 Hrs	1.050483	0.896756
6 Hrs	3.505585	1.739084
12 Hrs	3.580957	1.68124
24 Hrs	4.699045	0.642262
ACADM		
2 Hrs	0.821177	0.798203
4 Hrs	1.327261	0.790077
6 Hrs	1.752396	0.755447
12 Hrs	3.122123	2.092157
24 Hrs	0.629905	1.753868

ACOX1		
2 Hrs	0.53172	1.265926
4 Hrs	1.597867	1.48633
6 Hrs	1.298663	1.250723
12 Hrs	1.375194	1.520936
24 Hrs	1.343907	2.024645
MFn2		
2 Hrs	0.770359	2.201233
4 Hrs	1.161476	2.836852
6 Hrs	1.312131	1.520663
12 Hrs	1.284909	2.653902
24 Hrs	0.977946	3.283661
PPARGC1A		
2 Hrs	0.323974	1.041913
4 Hrs	1.06578	1.552372
6 Hrs	0.97147	1.046177
12 Hrs	1.738185	1.916893
24 Hrs	1.617468	1.581786
TFAM		
2 Hrs	0.774972	0.837845
4 Hrs	1.145149	0.694369
6 Hrs	1.604851	0.713822
12 Hrs	1.228752	0.804238
24 Hrs	0.798051	0.712819

4.6.2.2 *ACOX1* mRNA Levels were Altered in Response to Exposure Duration of Palmitic Acid

ACOX1 mRNA levels was significantly altered in response to exposure duration (p=0.0343, Table 14, Figure 15). Post Hoc testing was conducted for pairwise comparison between time points. Following treatment with a final media concentration of 800uM, ACOX1 mRNA levels at 4 hours was higher compared to 2 hours (p=0.0347) (Figure 15). Exposure to 800uM palmitic acid resulted in an increase in the fold change of *ACOX1* mRNA levels compared to untreated control cells between 4-24 hours post-exposure (FC=1.58, FC=1.30, FC=1.38, FC=1.34 respectively, Table 13). Similarly, exposure to 250uM palmitic acid resulted in an increase in the fold change of *ACOX1* mRNA levels compared to untreated control cells at all time points (2-24 hours) post exposure (FC=1.27, FC= 1.49, FC=1.25, FC=1.52, FC=2.02 respectively, Table 13).

Table 14: The Changes in *ACOX1* mRNA Levels Following Palmitic Acid Treatment

ACOX1 mRNA Levels	**Sum of Squares**	**Degrees of Freedom**	**Mean Squares**	**F (DFn, Dfd)**	**P-Value**
Interaction	0.6458	4	0.1614	F (4, 10) = 1.767	P=0.2120
Time	1.462	4	0.3656	F (4, 10) = 4.001	**P=0.0343**
Normalized Concentration (800uM vs. 250uM)	0.3927	1	0.3927	F (1, 10) = 4.297	P=0.0650

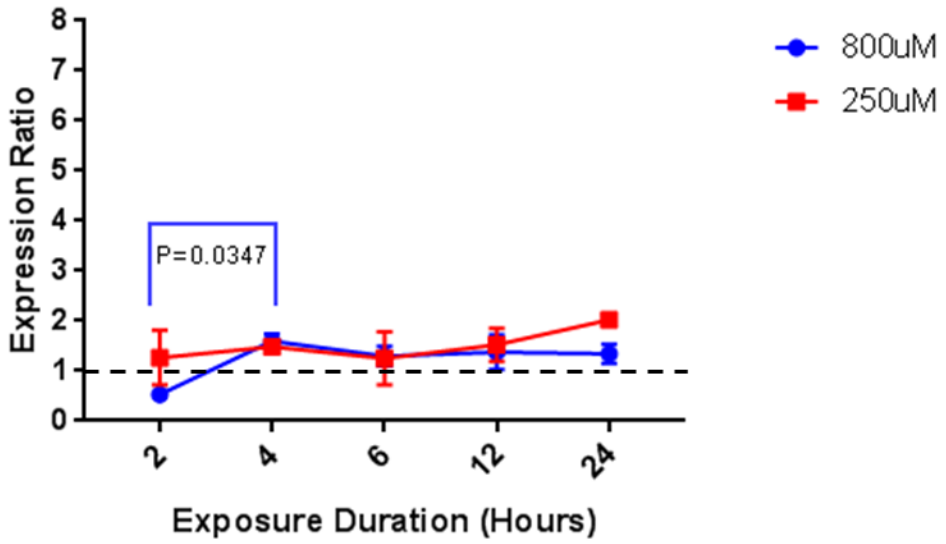

Figure 15: The Changes in *ACOX1* mRNA Levels Following Palmitic Acid Treatment. This assay quantified the effects of exposure to palmitic acid at a final media concentration of concentrations of 800uM and 250uM *ACOX1* mRNA levels. The expression ratio reflects the ratio of the expression in palmitic acid treated cells to that in control cells (untreated).

4.6.2.3 *MFn2* mRNA Levels were Altered in Response to Palmitic Acid

MFn2 mRNA levels were not significantly altered in response to exposure duration (2-24 hours) (p=0.9128), but were significantly altered in response to concentration (800uM or 250uM) (p=0.0425, Table 15, Figure 16). Following exposure to 800uM palmitic acid, the fold change of *MFn2* mRNA levels were higher than in untreated controls at 4, 6, and 12 hours post exposure (FC=1.16, FC=1.31, FC=1.28 respectively, Table 13). Exposure to 250uM palmitic acid resulted in an increase in the fold change of *MFn2* mRNA levels at 2, 4, 6, 12, and 24 hours post exposure (FC=2.2, FC=2.84, FC=1.52, FC=2.65, FC=3.28 respectively, Table 13).

Table 15: The Changes in *MFn2* mRNA Levels Following Palmitic Acid Treatment. Significant Values are in bold.

MFn2 mRNA Levels	Sum of Squares	Degrees of Freedom	Mean Squares	F (DFn, Dfd)	P-Value
Interaction	2.318	4	0.5794	F (4, 10) = 0.3203	P=0.8581
Time	1.695	4	0.4237	F (4, 10) = 0.2342	P=0.9128
Normalized Concentration (800uM vs. 250uM)	9.771	1	9.771	F (1, 10) = 5.401	**P=0.0425**

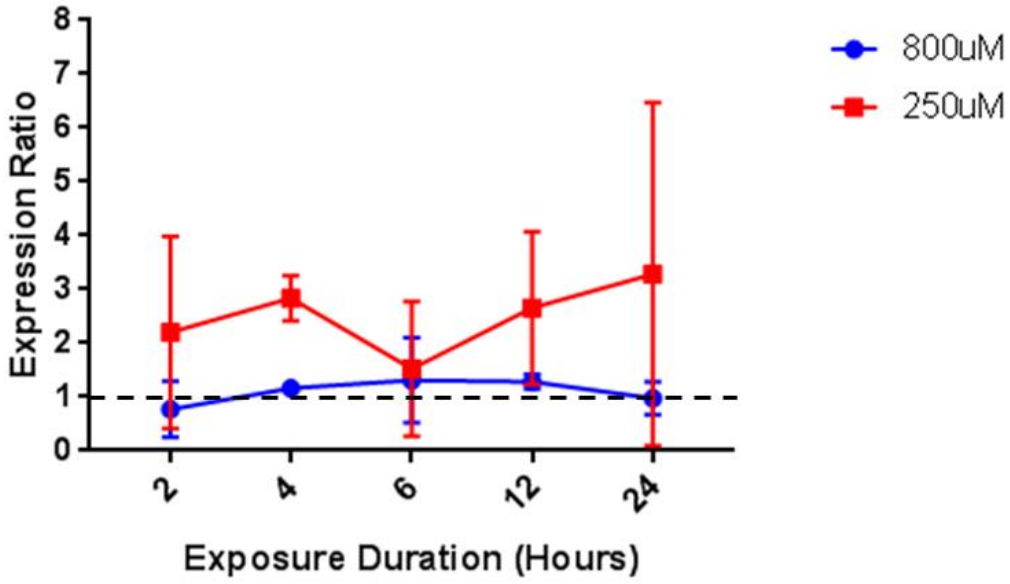

Figure 16: The Changes in MFn2 mRNA Levels Following Palmitic Acid Treatment. This assay quantified the effects of exposure to palmitic acid at a final media concentration of 800uM and 250uM on MFn2 mRNA levels. The expression ratio reflects the ratio of the expression in palmitic acid treated cells to that in control cells (untreated).

4.6.2.4 Palmitic Acid Exposure Concentration Significantly Alters *CPT-1a* and *MFn2* mRNA Levels

In cells treated with palmitic acid, while time had no effect, mRNA levels of *CPT-1a* (p=0.0133, Table 12) and *TFAM* (p=0.0425, Table 15) were significantly altered

between groups treated with 800uM and groups treated with 250uM of palmitic acid. mRNA levels of *ACADM* (p=0.5427), *ACOX1* (p=0.065), *PPARGC1A* (p=0.2795), and *TFAM* (p=0.2104) did not differ significantly following treatment with either 800uM or 250uM palmitic acid.

4.6.3 Effects of Butyric acid on Expression of Various Genes Involved in Lipid Metabolism and Mitochondrial Homeostasis

Exposure to butyric acid induced the changes in expression levels of various genes involved in lipid metabolism and mitochondrial homeostasis (Table 16).

Table 16: Fold Change (Treated/Untreated) of mRNA Levels Following Exposure to Butyric Acid

	800uM Fold Change	250uM Fold Change
CPT-1a		
2 Hrs	1.144945	3.275241
4 Hrs	2.029137	1.029654
6 Hrs	0.973847	1.126056
12 Hrs	2.280753	1.264445
24 Hrs	0.601463	0.28149
ACADM		
2 Hrs	1.191824	2.67251
4 Hrs	1.012704	0.96692
6 Hrs	0.70895	0.825525
12 Hrs	0.656759	1.075126
24 Hrs	0.523061	0.906256
ACOX1		
2 Hrs	1.246865	0.718782
4 Hrs	1.269885	1.252594

6 Hrs	1.211968	1.046252
12 Hrs	0.838764	0.719572
24 Hrs	0.250267	0.784734
MFn2		
2 Hrs	1.560946	1.091918
4 Hrs	1.329917	1.003651
6 Hrs	0.878492	0.674869
12 Hrs	0.671987	1.045038
24 Hrs	0.538004	1.285491
	800uM	250uM
PPARGC1A		
2 Hrs	1.721033	0.820751
4 Hrs	3.849921	1.271758
6 Hrs	4.069585	0.706412
12 Hrs	0.83962	0.723526
24 Hrs	0.456255	1.130618
TFAM		
2 Hrs	1.016926	2.422375
4 Hrs	0.870373	0.672085
6 Hrs	0.496014	0.491851
12 Hrs	0.62463	0.65441
24 Hrs	0.438365	0.52383

4.6.3.1 Butyric Acid Exposure Duration and Concentration Both Alter *ACADM* mRNA Levels

ACADM mRNA levels were significantly altered in response to exposure duration (2-24 hours) ($p=0.0128$) and in response to concentration (800uM or 250uM in the media) ($p=0.0331$, Table 17, Figure 17). Further Tukey Post Hoc testing was conducted for pairwise comparison between time points. Following treatment with 250uM butyric

acid, *ACADM* mRNA levels at 2 hours was higher compared to 4 hours (p=0.017), to 6 hours (p=0.01), to 12 hours (p=0.025), and to 24 hours (p=0.013, Figure 17, Figure 18). Following exposure to 800uM and 250uM butyric acid, the fold change in *ACADM* mRNA levels were increased compared to untreated control cells only at 2 hours (FC=1.19 and FC=2.67 respectively).

Table 17: The Changes in ACADM mRNA Levels Following Butyric Acid Treatment.

***ACADM* mRNA Levels**	**Sum of Squares**	**Degrees of Freedom**	**Mean Squares**	**F (DFn, Dfd)**	**P-Value**
Interaction	1.423	4	0.3557	F (4, 10) = 1.959	P=0.1770
Time	4.032	4	1.008	F (4, 10) = 5.554	**P=0.0128**
Normalized Concentration (800uM vs. 250uM)	1.107	1	1.107	F (1, 10) = 6.101	**P=0.0331**

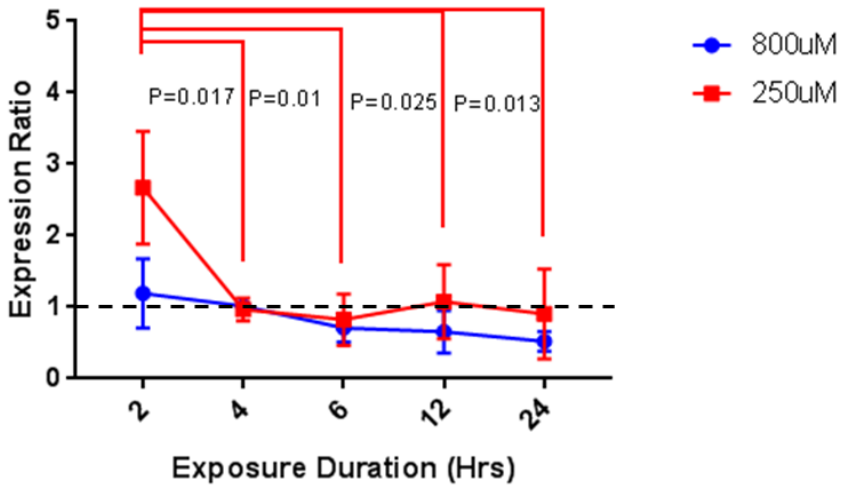

Figure 17: The Changes in ACADM mRNA Levels Following Butyric Acid Treatment. This assay quantified the effects of exposure to butyric acid at a final media concentration of 800uM and 250uM on expression ACADM mRNA levels. The expression ratio reflects the ratio of the expression in butyric acid treated cells to that in control cells (untreated).

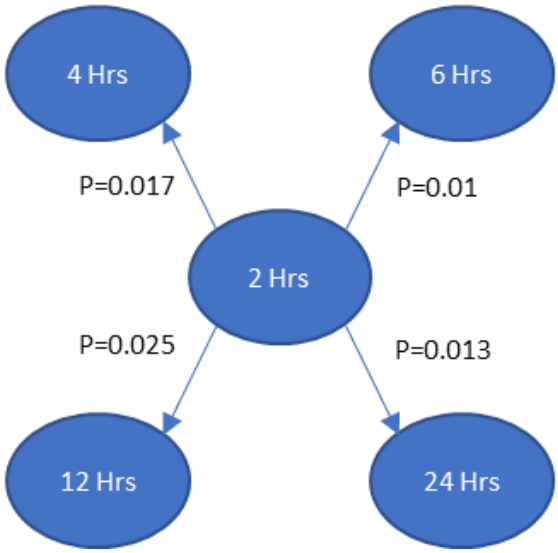

Figure 18: Pairwise Comparison of ACADM mRNA Levels Following Exposure to 250uM Butyric acid

4.6.3.2 Butyric Acid Exposure Duration Alters *ACOX1* mRNA Levels

ACOX1 mRNA levels were significantly altered in response to exposure duration (2-24 hours) (p=0.0362), but not in response to either 800uM or 250uM of butyric acid in the media) (p=0.6649, Table 18, Figure 19). Tukey Post Hoc testing was conducted for pairwise comparison between time points. Following treatment with 800uM of butyric acid, *ACOX1* mRNA levels at 24 hours were lower compared to that at 2 hours (p=0.045) and at 4 hours post-exposure (p=0.039) (Figure 19) (Figure 20), and were higher than in untreated controls at the time points of 2-6 hours post exposure (FC= 1.25, FC=1.27, FC=1.21 respectively) (Table 16). Interestingly, following exposure to 250uM butyric acid, *ACOX1* mRNA levels were higher than that in untreated controls at only one time point, 4 hours post exposure (FC=1.25) (Table 16).

Table 18: The Changes in *ACOX1* mRNA Levels Following Butyric Acid Treatment.

***ACOX1* mRNA Levels**	**Sum of Squares**	**Degrees of Freedom**	**Mean Squares**	**F (DFn, Dfd)**	**P-Value**
Interaction	0.589	4	0.1472	F (4, 10) = 1.675	P=0.2313
Time	1.38	4	0.345	F (4, 10) = 3.925	**P=0.0362**
Normalized Concentration (800uM vs. 250uM)	0.0175	1	0.0175	F (1, 10) = 0.1991	P=0.6649

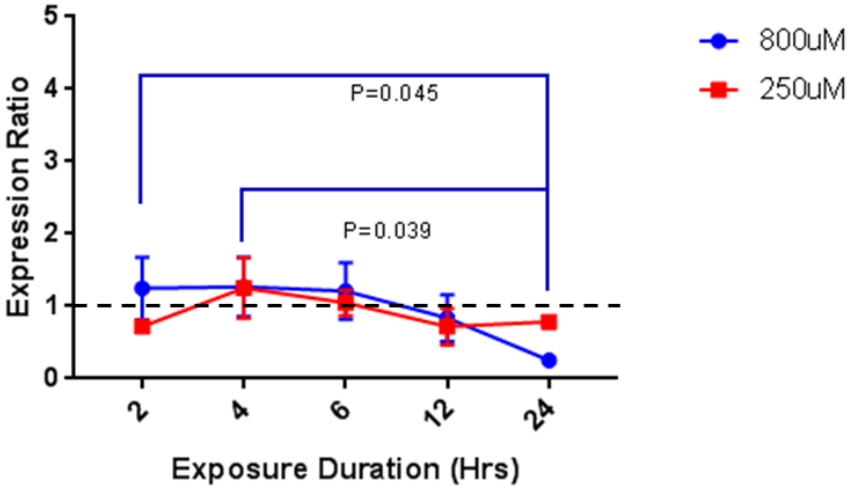

Figure 19: The Changes in *ACOX1* mRNA Levels Following Butyric Acid Treatment. This assay quantified the effects of exposure to butyric acid at a final media concentration of 800uM and 250uM on *ACOX1* mRNA levels. The expression ratio reflects the ratio of the expression in butyric acid treated cells to that in control cells (untreated).

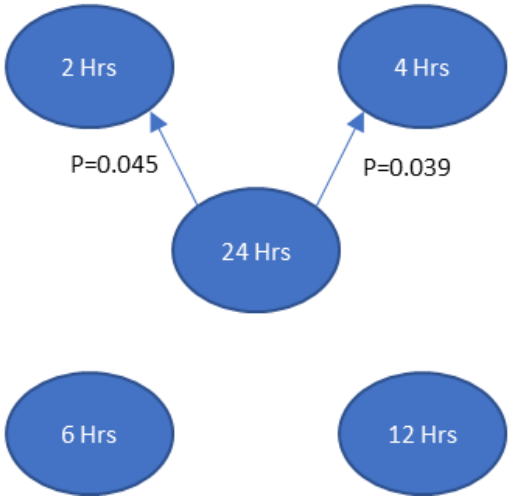

Figure 20: Pairwise Comparison of ACOX1 mRNA Levels Following Exposure to 800uM Butyric acid

4.6.3.3 Butyric Acid Exposure Duration and Concentration Both Altered *PPARGC1A* mRNA Levels

PPARGC1A mRNA levels were significantly altered by both exposure duration (2-24 hours) (p=0.0008) and concentration (800uM or 250uM) (p=0.0002, Table 19, Figure 21). ANOVA testing showed the interaction between these two factors to be significant and positive (F=11.44, p=0.0009). This suggests that *PPARGC1A* mRNA levels increases with an increase in exposure time as well as concentration over a short-term incubation. Post Hoc testing for exposure duration with 800uM butyric acid (Figure 21) showed that significant and maximum *PPARGC1A* mRNA levels were observed at 6 hours (FC=4.07), while treatments with a lowed butyric acid concentration (250uM) showed maximum *PPARGC1A* mRNA levels at 4 hours (FC=1.26, Figure 21). Following treatment with 800uM butyric acid, *PPARGC1A* mRNA levels at 6 hours was higher compared to 2 hours (p=0.0057), to 12 hours (p=0.0005), and to 24 hours (p=0.0002). Following treatment with 800uM butyric acid, *PPARGC1A* mRNA levels at 4 hours was higher compared to 2 hours (0.011), to 12 hours (p=0.0009), and to 24 hours (p=0.0003, Figure 21, Figure 22). Following exposure to 800uM butyric acid, the fold change in *PPARGC1A* mRNA levels were higher than in the untreated controls for 2-6 hours post exposure (FC=1.72, FC=3.85, FC=4.07 respectively, Table 16). Interestingly, following exposure to butyric acid in a final media concentration of 250uM, the *PPARGC1A* mRNA levels were higher than that in untreated controls at 4 and 24 hours post exposure (FC=1.27 and FC=1.13 respectively, Table 16).

Table 19: The Changes in PPARGC1A mRNA Levels Following Butyric Acid Treatment.

PPARGC1A mRNA Levels	Sum of Squares	Degrees of Freedom	Mean Squares	F (DFn, Dfd)	P-Value
Interaction	11.34	4	2.835	F (4, 10) = 11.44	**P=0.0009**
Time	11.86	4	2.964	F (4, 10) = 11.96	**P=0.0008**
Normalized Concentration (800uM vs. 250uM)	7.896	1	7.896	F (1, 10) = 31.85	**P=0.0002**

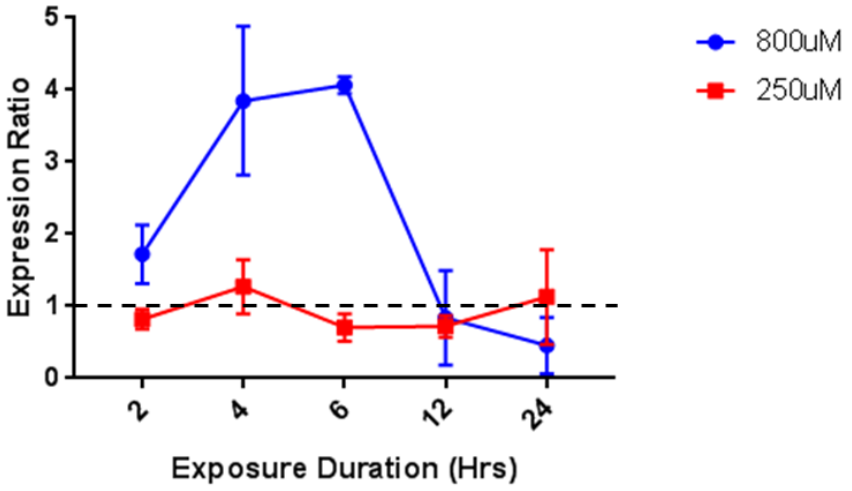

Figure 21: The Changes in PPARGC1A mRNA Levels Following Butyric Acid Treatment. This assay quantified the effects of exposure to butyric acid at a final media concentration of 800uM and 250uM on *PPARGC1A* mRNA levels. The expression ratio reflects the ratio of the expression in butyric acid treated cells to that in control cells (untreated).

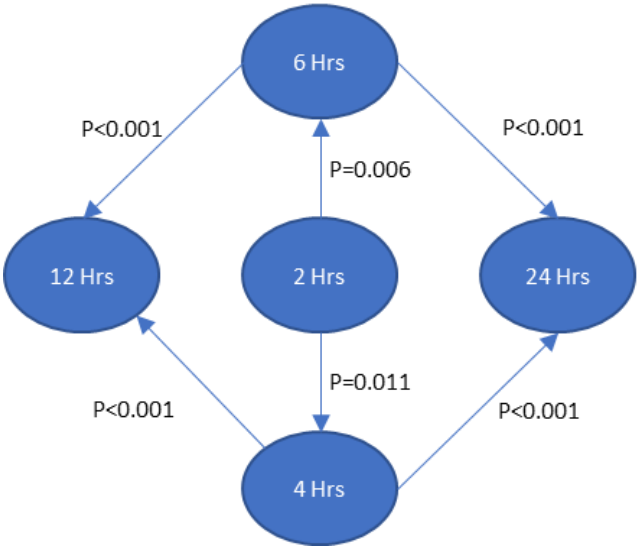

Figure 22: Pairwise Comparison of PPARGC1A mRNA Levels Following Exposure to 800uM Butyric Acid

4.6.3.4 Butyric Acid Exposure Duration and Concentration Altered *TFAM* mRNA Levels

TFAM mRNA levels were significantly altered in response to exposure duration and concentration (p=0.0006, Table 20) as indicated by a positive and significant interaction (F=5.087, p=0.0169, Table 20). Further, exposure duration alone had a positive and significant effect on TFAM mRNA levels (F=12.94, p=0.0006), while concentration did not have a significant effect. Additional post hoc comparison revealed that *TFAM* mRNA levels were increased at 2 hours compared to 4 hours (p=0.0008), to 6 hours (p=0.0004), to 12 hours (p=0.0008), and to 24 hours (p=0.0004) following exposure to 250uM (Figure 23, Figure 24). Following exposure to 250uM butyric acid, the *TFAM* mRNA levels were higher than that in untreated controls at 2 hours post exposure (FC= 2.42) (Table 16).

Table 20: The Changes in *TFAM* mRNA Levels Following Butyric Acid Treatment.

***TFAM* mRNA Levels**	**Sum of Squares**	**Degrees of Freedom**	**Mean Squares**	**F (DFn, Dfd)**	**P-Value**
Interaction	1.675	4	0.4188	F (4, 10) = 5.087	**P=0.0169**
Time	4.262	4	1.065	F (4, 10) = 12.94	**P=0.0006**
Normalized Concentration (800uM vs. 250uM)	0.3476	1	0.3476	F (1, 10) = 4.222	P=0.0670

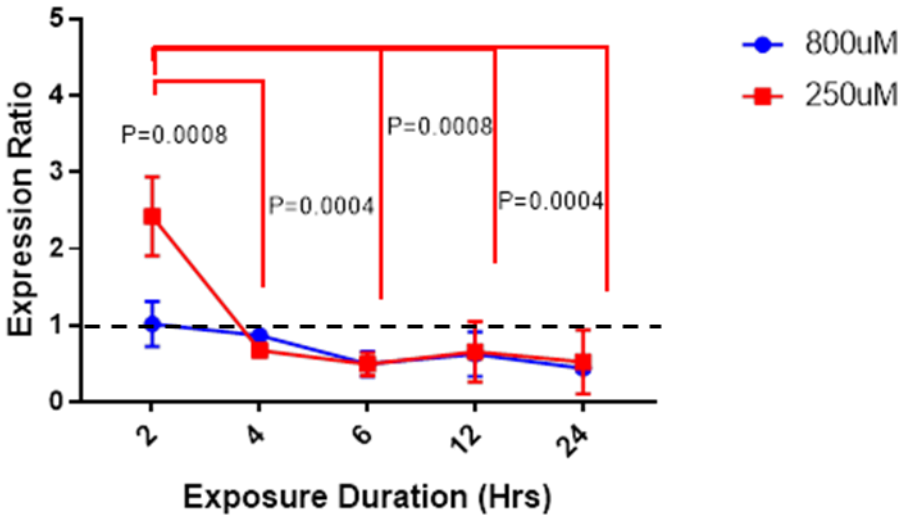

Figure 23: The Changes in *TFAM* mRNA Levels Following Butyric Acid Treatment. This assay quantified the effects of exposure to butyric acid at a final media concentration of 800uM and 250uM on *TFAM* mRNA levels. The expression ratio reflects the ratio of the expression in butyric acid treated cells to that in control cells (untreated).

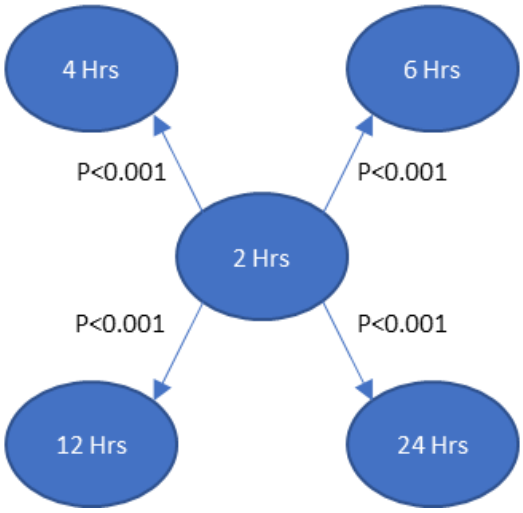

Figure 24: Pairwise Comparisons of TFAM mRNA Levels Following Exposure to 250uM Butyric acid

4.6.3.5 Butyric Acid Exposure Concentration Significantly Alters *ACADM* and *PPARGC1A* mRNA Levels

In cells treated with butyric acid, mRNA levels of *ACADM* (p=0.0331, Table 17) and *PPARGC1A* (p=0.0002, Table 19) were significantly altered between groups treated with a final media concentration of 800uM and groups treated with a final media concentration of 250uM. mRNA levels of *CPT-1a* (p=0.0977), *ACOX1* (p=0.665), *MFn2* (p=0.921), and *TFAM* (p=0.0001) did not differ significantly following treatment with either 800uM or 250uM butyric acid.

CHAPTER FIVE: DISCUSSION

5.1 Exposure to Fatty Acids May Influence Lipid Metabolism

As the epidemic of NAFLD continues to grow, more emphasis on understanding of molecular underpinnings behind its etiology and progression to NASH is necessary. This study was undertaken to elucidate the effects of exposure to various lipid species on both the cellular and mitochondrial functions of hepatocytes, in a simple *in vitro* model of NAFLD. As the mitochondria serve as the main site of lipid breakdown, we hypothesized that challenging of hepatocytes with lipids would result in either alteration in ratio of mitochondrial to nuclear DNA, or changes in expression of genes involved in mitochondrial homeostasis and lipid metabolism, or both. Our hope was that quantitative measures of hepatocyte responses would provide insight into how short term (2-24 hours) exposure to various fatty acid species influence mitochondrial functioning, and potentially to the lipid-promoted development of NAFLD and associated co-morbidities.

In this study, we showed that a short-term exposure (4 hours) to oleic acid in a final media concentration of 800uM led to an increase in *ACADM* mRNA levels (Table 10). This mRNA encodes medium-chain specific acyl-Coenzyme A dehydrogenase, belonging to the family of enzymes that catalyze the initial step of the β-oxidation pathway. Importantly, expression of mRNA encoding carnitine palmitoyltransferase 1a (*CPT-1a*) (Figure 12), the rate limiting step in the mitochondrial import of fatty acids,

was decreased, while the levels of mRNAs encoding a transcriptional activator of *CPT-1a* (*PPARGC1A*) (Table 10) and peroxisomal acyl-coenzyme A oxidase (*ACOX1*) (Table 10), the first enzyme in the peroxisomal fatty acid β-oxidation pathway, were not altered. These observations suggest that oleic acid may selectively modulate β-oxidation in the mitochondria, but not in peroxisomes.

The observed decrease in *CPT-1a* encoding mRNA may be due to suppression of peroxisome proliferator activated receptor α (*PPARα*) and PGC-1*α.* PPARα is a nuclear receptor which plays a role in many functions including both mitochondrial and peroxisomal β-oxidation and transport of fatty acids (See Contreras et al., 2013 for review). In *PPARα*-deficient mice, an increase in hepatic lipid accumulation was observed following either a high-fat diet or fasting, indicating the role of this regulator in intrahepatic oxidation of fatty acids (Kersten et al., 1999).

Peroxisome proliferator-activated receptor γ coactivator 1, PGC-*1α,* (encoded by *PPARGC1A*) serves as a master regulator of gene expression in mitochondria (See Handschin and Spiegelman, 2006 for review). Interestingly, overexpression of PGC-1*α* in cultured myotubes enhances mitochondrial oxidative capacity by increasing the levels of mRNAs encoded by *ACADM*, *ACADML*, *ACADCL*, and *CPT-1b*, the muscle isoform of carnitine palmitoyltransferase (Espinoza et al., 2010). It is also worthwhile to note that stimulation of CPT-1a in rat livers by PGC-1*α* and PPARα are independent and through different locations on the CPT-1a gene (Song et al., 2010). Comparative analysis of the functions of PPARα in humans and mice showed that of the 125 genes co-regulated by PPARα, many are involved in processing of hepatic lipids, including fatty acid oxidation,

ketogenesis, fatty acid binding and activation, and fatty acid uptake, highlighting PPARα as a master regulator of hepatic metabolism (Rakhshandehroo et al., 2009). STRING protein interaction network centered on *PPARGC1A* and *PPARα* highlights the role of genes studies here as important regulators of metabolism (Figure 25).

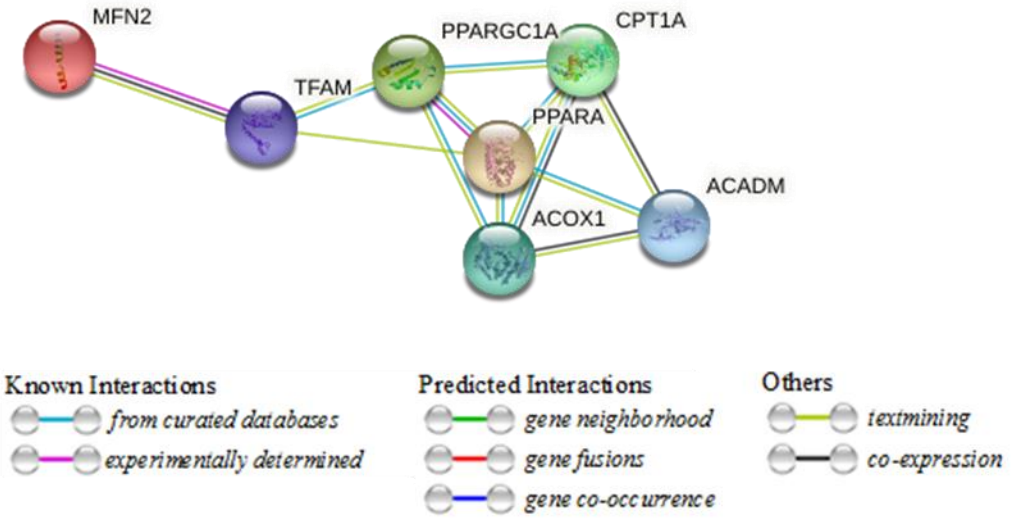

Figure 25: The Dynamic Metabolic Control of PPARα and PPARGC1α. (Adapted from STRING v10.Szklarczyk et al., 2015)

We also performed a comparison of these results to that of short term exposure with either palmitic acid or butyric acid (800uM in the media). In HepG2 cells exposed to palmitic acid at 4 hours, the levels *CPT-1a* (Figure 14) and *PPARGC1A* encoding mRNA (Table 13) levels were unchanged, while increases in *ACOX1* (Figure 15) and *ACADM* (Table 13) mRNA levels were observed, suggesting an increase in both mitochondrial and peroxisomal beta-oxidation. These results coupled with no change in lipid

accumulation at 4 hours highlights substantial similarity in response of mitochondria to palmitic and oleic acid. However, the increase in *ACOX1* mRNA levels (Figure 15) following palmitic acid treatment highlights the possible use of both mitochondrial and peroxisomal pathways in order to prime the cells and increase their capacity to breakdown long chain saturated acids such as palmitic acid. On the other hand, short term (4 hours) exposure to 800uM butyric acid showed a pattern different to one observed in experimental treatment with the same type of cells. No change in lipid accumulation was observed as previously (Figure 8). However, increased *CPT-1a* (Table 16), *PPARGC1A* (Figure 21), and *ACOX1* mRNA levels (Figure 19) were seen, with no increase in *ACADM* mRNA levels (Figure 17), indicating increased levels of mitochondrial transport, but not oxidation. This observation is interesting, since short chain FFA can cross the mitochondrial membrane independently of the carnitine shuttle. It is of importance to note that dietary supplementation with butyrate results in stimulation of fibroblast growth factor 21 (FGF21), which is known to stimulate the PGC-1*α* protein (Li et al., 2012; Potthoff et al., 2009; Raso et al., 2013). Our results are in accordance with activation of *PPARGC1A* in the presence of butyric acid.

Interestingly, treatment with a lower dose of fatty acids (250uM in the media) resulted in a different pattern of lipid accumulation and lipid processing as compared to the treatment with 800uM of same compound. Following exposure to oleic acid at 6 hours, an increase in *CPT-1a* and *ACADM* mRNA levels (Table 10) was observed, while the mRNA levels of *ACOX1* (Table 10), and *PPARGC1A* (Table 10) were unchanged. At 12 hours, however, *CPT-1a* (Figure 12) and *ACADM* mRNA levels (Table 10) were

also increased. When cells were treated with palmitic acid, similar trends were revealed, with increased *CPT-1a* mRNA levels (Figure 14) at 6 hours, followed by an increase in *ACADM* mRNA levels (Table 13) at 12 hours. For butyric acid, an increase of *CPT-1a* mRNA levels (Table 16) was observed at 6 hours, while an increase in *ACADM* mRNA levels (Figure 17) was detected at 2 hours, but was not changed compared to the non-exposed control cells at 4 and decreased at 6 hours. No changes in *ACADM* mRNA levels were seen. This is expected as the enzymatic action of ACADM is specific to medium chain fatty acids, and does not use short-chain fatty acids as a substrate. The drops in mRNA levels of *ACADM* expression relative to 2 hrs could indicate down-regulation of *ACADM* mediated pathways in the presence of butyric acid (FC=1 at 4 hours vs. 1.19 at 2 hours).

5.2 Effects of Exposure to Fatty Acids on the Ratio of Mitochondrial to Nuclear DNA and Oxidative Stress

During aerobic respiration, the mitochondrial respiratory chain uses oxygen as the final electron acceptor, hereby, potentially generating reactive oxygen species (ROS) (See Murphy, 2009 for review). As oxygen is reduced one electron at a time, stable intermediates are formed. In case of an imbalance between formation and quenching through antioxidants, a buildup of ROS occurs (Turrens, 2003). Preservation of the oxidative environment is crucial to proper functioning of mitochondria and to cellular homeostasis, which can be perturbed by the presence of fatty acids. Previous literature has shown that in cultured human hepatocytes, oxidative stress is induced by free fatty

acids following incubation for 7 days with a mixture of linoleic, arachidonic, oleic, myristic, palmitic, and stearic acids (Soardo et al., 2011). Following incubation with a mix of these fatty acids, a decrease in intracellular glutathione (iGSH) pool was noted, while incubation with excess of GSH alleviated oxidative stress (Soardo et al., 2011).

Due to the close proximity of mitochondrial DNA to ROS, oxidative damage of mtDNA is common. The primary cellular response to this damage is elimination of the damaged DNA along with increased replication of mtDNA (Shokolenko et al., 2009). Several studies have shown a strong and positive correlation between the levels of oxidative stress and an increase in mtDNA (Lee et al., 2000, 2002). Notably, in a study by Lee et al., treatment of lung fibroblasts with sub-lethal levels of H_2O_2, a known reactive oxygen species, led to an increase in oxidative stress, and an increase in the amount of mtDNA independent of cell-cycle control (Lee et al., 2000). Our study shows an increase in the ratio of mitochondrial DNA to nuclear DNA at 4 hours following treatment with palmitic acid (800uM in the media) (Figure 10). These results are in agreement with the studies that have reported that increased levels of free fatty acids induce oxidative stress and a subsequent increase in ratio of mitochondrial to nuclear DNA to compensate for damaged mitochondrial DNA (Lee et al., 2000; Lee et al., 2002).

While the regulation of mitochondrial DNA (mtDNA) copy number is not well understood, mitochondrial transcription factors encoded in the nucleus play a central role. Interestingly, exposure concentration (800uM or 250uM) following treatment with oleic ($p=0.0007$, Figure 13, Table 11) significantly altered *TFAM* mRNA levels with an overall decrease seen following both treatment concentrations. However, following exposure to

250uM butyric acid, *TFAM* mRNA levels were significantly altered (p=0.0006, Figure 23, Table 20) with increased mRNA levels, relative to unexposed control cells, at 2 hours, followed by a decrease from 4 to 24 hours. Although *TFAM* mRNA levels changed, there was no significant concomitant change in the ratio of mitochondrial to nuclear DNA upon exposure to butyric acid. This may be due to cells being primed for a high energy response by an upregulation of gene transcription.

An increase in the fold-change of ratio of mitochondrial to nuclear DNA was observed after exposure to oleic acid and palmitic acids (Figure 10 & Figure 11), with the higher treatment concentration (800uM) eliciting an increase in mitochondria DNA at an earlier time point (≤ 6 hours) than the lower treatment concentration (250uM) of the two long-chain lipids. Exposure to a higher concentration of stressors may cause oxidative stress of larger magnitudes, leading to earlier mitochondrial DNA damage, and an earlier onset of the stress response.

Interestingly, the increase in the ratio of mitochondrial to nuclear DNA occurs earlier for palmitic acid than for oleic acid, in agreement with known proapoptotic effects of palmitic acid (Ricchi et al., 2009). In pancreatic β cells, palmitic acid may cross the cellular membrane when present in high concentrations. In previously described experiments, the treatment with palmitic acid led to an increase in ROS levels 2.5 fold compared to controls, indicating the pro-oxidative properties of palmitic acid (Xu et al., 2013). Comparison of ROS production as measured in experiments with carbon-18 fatty acids that differed in saturation showed a different response in Jurkat and Raji cells. In

particular, exposures to either linoleic acid (C18:2) or oleic acid (C18:1) resulted in the highest levels of ROS production (Cury-Boaventura and Curi, 2005).

Treatment with palmitic acid in a final media concentration of 800uM resulted in a significant increase in mtDNA mass at 4 hours ($p=0.0296$), while treatment with 250uM resulted in an increase in mtDNA mass at 6 hours (not significant) (Figure 11). The concentration of palmitic acid may have differing effects on ROS-induced mtDNA damage. Treatment of HepG2 cells with 800uM palmitic acid resulted in noticeable apoptosis at 24 hours (mean = 1463.7 U/L), while no apoptosis was seen across any other time point or any other lipid treatment (data not shown). Exposure to high levels of palmitic acid (800uM) may have induced severe oxidative damage to the mtDNA which the cell could not compensate for by increasing replication, thereby leading to apoptosis.

Similar changes in mtDNA mass were observed following treatments with oleic acid. At 800uM oleic acid, an increase in mtDNA was detected at an earlier time point (6 hours) than upon treatment with 250uM (12 hours) (Figure 9). The increase in mtDNA masses was transient as treatment with 800uM oleic acid resulted in a subsequent decrease, while treatment with 250uM resulted in increased mtDNA mass at 24 hours. Treatment with 800uM palmitic acid resulted in no overall change, fold-change around 1, at 24 hours, however treatment with 250uM resulted in decreased mtDNA mass compared to controls after 24 hours (Figure 10). Comparison of the treatments with oleic acid and palmitic acid showed a larger increase in mtDNA following treatment with 800uM oleic acid as compared to 800uM palmitic acid. However, as no significant

apoptotic events were observed, this could be due to the ability of oleic acid to modulate oxidative stress and trigger oxidative phosphorylation.

Interestingly, mitofusin-2 (*MFn2*) mRNA levels were altered in response to palmitic acid exposure concentration, but not exposure duration ($p=0.0425$, Table 15, Figure 16). Mitochondria are not static, stand-alone organelles, but form a dynamic network of fusions and fissions. Mitochondrial fissions are necessary for meeting energy demands of growing and dividing cells (Youle and van der Bliek, 2012). However, mitochondrial fissions can also occur in the presence of stressors, thus, preparing the mitochondria for mitophagy and apoptosis (Barbour and Turner, 2014). Exposures to increasing levels of palmitate result in increased levels of mitochondrial fission in cultured muscle cells (Jheng et al., 2012). In our study, exposures to 250uM palmitic acid resulted in significantly increased mRNA levels of *MFn2*, indicating possible changes in the mitochondrial architecture (Figure 16).

On the other hand, mitochondrial fusion can be used by mitochondria in a "pro-survival" mechanism through increased resistance to apoptosis and mitophagy following mitochondrial stress (Barbour and Turner, 2014; Youle and van der Bliek, 2012). Elucidation of mitochondrial fusion and fission levels following treatment would provide a better understanding of how exogenous fatty acids influence mitochondrial health and architecture.

In summary, a differential response of mitochondria to fatty acids reveals not all fatty acid classifications act similarly. HepG2 cells were treated with three fatty acid species that differed in length and saturation (

Figure 26). Palmitic acid resulted in an increase in systems dealing with copy number and fusion, implying greater mitochondrial stress as well as increased apoptosis. Oleic acid treatment resulted in a decrease in mitochondrial copy number regulation as well as a resistance to fatty acid import at either concentration. Butyric acid treatment resulted in increased lipid accumulation and mitochondrial beta-oxidation (Table 21).

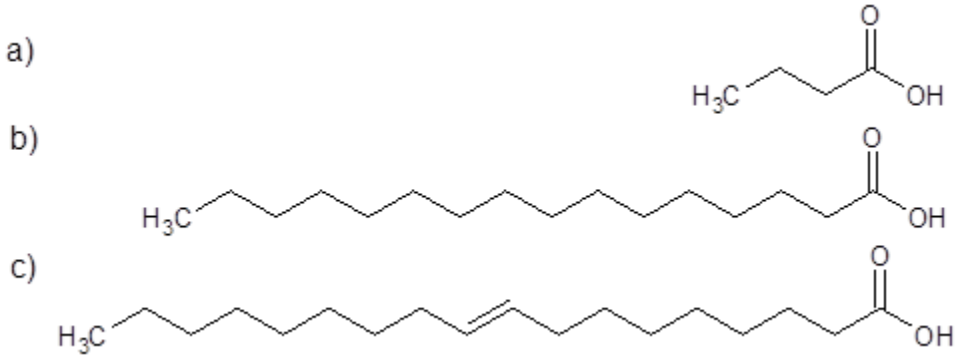

Figure 26: Fatty Acid Species used in this Assay: a) Butyric Acid, b) Palmitic Acid, c) Oleic Acid

Table 21: Summary of Observations

Oleic	Palmitic	Butyric
CPT-1a ↓	Lipid Accumulation ↓	Lipid Accumulation ↑
TFAM ↓	Apoptosis ↑	ACADM ↑
	Mitochondrial DNA Ratio ↕	ACOX1 ↓
	CPT-1a ↑	TFAM ↕
	ACOX1 ↑	PPARGC1A ↕
	MFn2 ↑	

As our study used a cell culture model, complete elucidation of the role of fatty acids on mitochondrial and cellular functions was not possible. Limitations in this study included not being able to measure the proportion of fatty acids left in the media to the end of the treatment period, which precluded us from quantifying the amounts absorbed. Further work in better models, including those that involve multiple cell types are necessary. One such model co-cultured primary hepatocytes with hepatic stellate cells and macrophages, and then exposed them to media containing high levels of NASH-associated-metabolites, including glucose, insulin, and free fatty acids (Feaver et al., 2016). A second model, using microfluidics, mimics the liver sinusoid and the hepatic microvasculature, allowing for a better representation of hepatocytes following free fatty acid supplementation (Gori et al., 2016).

Secondly, the majority of animal models for NAFLD and NASH are either rats or mice, with differing diets, leading to differences in the results, and difficulties in interpretation. Comparison of two rat strains, Sprague-Dawley and Wistar, following a high-fat diet, showed that the Sprague-Dawley strain developed steatosis, while the Wistar rats did not (Lieber et al., 2004; Romestaing et al., 2007; Takahashi et al., 2012). Standardization of the diet or mouse strains would provide a consistent basis for which only the supplemented fatty acids would change, reducing the number of confounding variables.

Overall, this study profiled the dynamic and complex response of hepatocytes to exogenous free fatty acids. Differences in expression levels of genes involved in beta-oxidation rates brings some insights into a dynamic interplay of fatty acids, their

catabolic products, and transcriptional regulation in human hepatocytes. Lipid overload causes aberrations of these processes, and results in increased oxidative stress, and mitochondrial damage. To further elucidate this complex system, tracking of fatty acids, by radiolabeling or other means, as well as using primary hepatocytes, or in *in vitro* multicellular systems, similar to the ones described above, is necessary.

REFERENCES

Ahmadian, M., Duncan, R.E., Jaworski, K., Sarkadi-Nagy, E., and Sul, H.S. (2007). Triacylglycerol metabolism in adipose tissue. Future Lipidol 2, 229–237.

Ameer, F., Scandiuzzi, L., Hasnain, S., Kalbacher, H., and Zaidi, N. (2014). De novo lipogenesis in health and disease. Metabolism 63, 895–902.

Anstee, Q.M., and Goldin, R.D. (2006). Mouse models in non-alcoholic fatty liver disease and steatohepatitis research. Int J Exp Pathol 87, 1–16.

Aon, M.A., Bhatt, N., and Cortassa, S.C. (2014). Mitochondrial and cellular mechanisms for managing lipid excess. Front Physiol 5.

Arendt, B.M., Comelli, E.M., Ma, D.W.L., Lou, W., Teterina, A., Kim, T., Fung, S.K., Wong, D.K.H., McGilvray, I., Fischer, S.E., et al. (2015). Altered hepatic gene expression in nonalcoholic fatty liver disease is associated with lower hepatic n-3 and n-6 polyunsaturated fatty acids. Hepatology 61, 1565–1578.

Barbour, J.A., and Turner, N. (2014). Mitochondrial Stress Signaling Promotes Cellular Adaptations. International Journal of Cell Biology 2014, e156020.

Barr, J., Alonso, C., Vázquez-Chantada, M., Cormenzana, M.P.-, Mayo, R., Galán, A., Caballería, J., Martín-Duce, A., Tran, A., Wagner, C., et al. (2010). Liquid

Chromatography-Mass Spectrometry (LC/MS)-based parallel metabolic profiling of human and mouse model serum reveals putative biomarkers associated with the progression of non-alcoholic fatty liver disease. J Proteome Res 9, 4501–4512.

Browning, J.D., Szczepaniak, L.S., Dobbins, R., Nuremberg, P., Horton, J.D., Cohen, J.C., Grundy, S.M., and Hobbs, H.H. (2004). Prevalence of hepatic steatosis in an urban population in the United States: Impact of ethnicity. Hepatology 40, 1387–1395.

Chalasani, N., Younossi, Z., Lavine, J.E., Diehl, A.M., Brunt, E.M., Cusi, K., Charlton, M., and Sanyal, A.J. (2012). The diagnosis and management of non-alcoholic fatty liver disease: Practice Guideline by the American Association for the Study of Liver Diseases, American College of Gastroenterology, and the American Gastroenterological Association. Hepatology 55, 2005–2023.

Charos, A.E., Reed, B.D., Raha, D., Szekely, A.M., Weissman, S.M., and Snyder, M. (2012). A highly integrated and complex PPARGC1A transcription factor binding network in HepG2 cells. Genome Res 22, 1668–1679.

Cinti, D.L., Cook, L., Nagi, M.N., and Suneja, S.K. (1992). The fatty acid chain elongation system of mammalian endoplasmic reticulum. Prog. Lipid Res. 31, 1–51.

Contreras, A.V., Torres, N., and Tovar, A.R. (2013). PPAR-α as a Key Nutritional and Environmental Sensor for Metabolic Adaptation. Adv Nutr 4, 439–452.

Cury-Boaventura, M.F., and Curi, R. (2005). Regulation of reactive oxygen species (ROS) production by C18 fatty acids in Jurkat and Raji cells. Clinical Science 108, 245–253.

Doege, H., Baillie, R.A., Ortegon, A.M., Tsang, B., Wu, Q., Punreddy, S., Hirsch, D., Watson, N., Gimeno, R.E., and Stahl, A. (2006). Targeted deletion of FATP5 reveals multiple functions in liver metabolism: alterations in hepatic lipid homeostasis. Gastroenterology 130, 1245–1258.

Donnelly, K.L., Smith, C.I., Schwarzenberg, S.J., Jessurun, J., Boldt, M.D., and Parks, E.J. (2005). Sources of fatty acids stored in liver and secreted via lipoproteins in patients with nonalcoholic fatty liver disease. J. Clin. Invest. 115, 1343–1351.

Ehehalt, R., Füllekrug, J., Pohl, J., Ring, A., Herrmann, T., and Stremmel, W. (2006). Translocation of long chain fatty acids across the plasma membrane – lipid rafts and fatty acid transport proteins. Mol Cell Biochem 284, 135–140.

Ekstrand, M.I., Falkenberg, M., Rantanen, A., Park, C.B., Gaspari, M., Hultenby, K., Rustin, P., Gustafsson, C.M., and Larsson, N.-G. (2004). Mitochondrial transcription factor A regulates mtDNA copy number in mammals. Hum Mol Genet 13, 935–944.

Espinoza, D.O., Boros, L.G., Crunkhorn, S., Gami, H., and Patti, M.-E. (2010). Dual modulation of both lipid oxidation and synthesis by peroxisome proliferator-activated receptor-γ coactivator-1α and -1β in cultured myotubes. FASEB J 24, 1003–1014.

Eynon, N., Morán, M., Birk, R., and Lucia, A. (2011). The champions' mitochondria: is it genetically determined? A review on mitochondrial DNA and elite athletic performance. Physiol. Genomics 43, 789–798.

Faergeman, N.J., DiRusso, C.C., Elberger, A., Knudsen, J., and Black, P.N. (1997). Disruption of the Saccharomyces cerevisiae homologue to the murine fatty acid transport protein impairs uptake and growth on long-chain fatty acids. J. Biol. Chem. 272, 8531–8538.

Fahy, E., Subramaniam, S., Murphy, R.C., Nishijima, M., Raetz, C.R.H., Shimizu, T., Spener, F., Meer, G. van, Wakelam, M.J.O., and Dennis, E.A. (2009). Update of the LIPID MAPS comprehensive classification system for lipids. J. Lipid Res. 50, S9–S14.

Fahy, E., Cotter, D., Sud, M., and Subramaniam, S. (2011). Lipid classification, structures and tools. Biochim Biophys Acta 1811, 637–647.

Feaver, R.E., Cole, B.K., Lawson, M.J., Hoang, S.A., Marukian, S., Blackman, B.R., Figler, R.A., Sanyal, A.J., Wamhoff, B.R., and Dash, A. (2016). Development of

an in vitro human liver system for interrogating nonalcoholic steatohepatitis. JCI Insight 1.

Fellmann, L., Nascimento, A.R., Tibiriça, E., and Bousquet, P. (2013). Murine models for pharmacological studies of the metabolic syndrome. Pharmacology & Therapeutics 137, 331–340.

Gastaldi, G., Russell, A., Golay, A., Giacobino, J.-P., Habicht, F., Barthassat, V., Muzzin, P., and Bobbioni-Harsch, E. (2007). Upregulation of peroxisome proliferator-activated receptor gamma coactivator gene (PGC1A) during weight loss is related to insulin sensitivity but not to energy expenditure. Diabetologia 50, 2348–2355.

Gorden, D.L., Ivanova, P.T., Myers, D.S., McIntyre, J.O., VanSaun, M.N., Wright, J.K., Matrisian, L.M., and Brown, H.A. (2011). Increased Diacylglycerols Characterize Hepatic Lipid Changes in Progression of Human Nonalcoholic Fatty Liver Disease; Comparison to a Murine Model. PLoS One 6.

Gori, M., Simonelli, M.C., Giannitelli, S.M., Businaro, L., Trombetta, M., and Rainer, A. (2016). Investigating Nonalcoholic Fatty Liver Disease in a Liver-on-a-Chip Microfluidic Device. PLOS ONE 11, e0159729.

Handschin, C., and Spiegelman, B.M. (2006). Peroxisome proliferator-activated receptor gamma coactivator 1 coactivators, energy homeostasis, and metabolism. Endocr. Rev. 27, 728–735.

Houten, S.M., and Wanders, R.J.A. (2010). A general introduction to the biochemistry of mitochondrial fatty acid β-oxidation. J Inherit Metab Dis 33, 469–477.

Jheng, H.-F., Tsai, P.-J., Guo, S.-M., Kuo, L.-H., Chang, C.-S., Su, I.-J., Chang, C.-R., and Tsai, Y.-S. (2012). Mitochondrial Fission Contributes to Mitochondrial Dysfunction and Insulin Resistance in Skeletal Muscle. Mol. Cell. Biol. 32, 309–319.

Kerner, J., and Hoppel, C. (2000). Fatty acid import into mitochondria. Biochim. Biophys. Acta 1486, 1–17.

Kersten, S., Seydoux, J., Peters, J.M., Gonzalez, F.J., Desvergne, B., and Wahli, W. (1999). Peroxisome proliferator–activated receptor α mediates the adaptive response to fasting. J Clin Invest 103, 1489–1498.

Kucera, O., and Cervinkova, Z. (2014). Experimental models of non-alcoholic fatty liver disease in rats. World J Gastroenterol 20, 8364–8376.

Larsson, N.G., Wang, J., Wilhelmsson, H., Oldfors, A., Rustin, P., Lewandoski, M., Barsh, G.S., and Clayton, D.A. (1998). Mitochondrial transcription factor A is necessary for mtDNA maintenance and embryogenesis in mice. Nat. Genet. 18, 231–236.

Lee, H.C., Yin, P.H., Lu, C.Y., Chi, C.W., and Wei, Y.H. (2000). Increase of mitochondria and mitochondrial DNA in response to oxidative stress in human cells. Biochem J 348, 425–432.

Lee, H.-C., Yin, P.-H., Chi, C.-W., and Wei, Y.-H. (2002). Increase in mitochondrial mass in human fibroblasts under oxidative stress and during replicative cell senescence. J. Biomed. Sci. 9, 517–526.

Leers, M.P., Kölgen, W., Björklund, V., Bergman, T., Tribbick, G., Persson, B., Björklund, P., Ramaekers, F.C., Björklund, B., Nap, M., et al. (1999). Immunocytochemical detection and mapping of a cytokeratin 18 neo-epitope exposed during early apoptosis. J. Pathol. 187, 567–572.

Legrand, P., and Rioux, V. (2010). The Complex and Important Cellular and Metabolic Functions of Saturated Fatty Acids. Lipids 45, 941–946.

Leonard, A.E., Pereira, S.L., Sprecher, H., and Huang, Y.-S. (2004). Elongation of long-chain fatty acids. Prog. Lipid Res. 43, 36–54.

Li, H., Gao, Z., Zhang, J., Ye, X., Xu, A., Ye, J., and Jia, W. (2012). Sodium Butyrate Stimulates Expression of Fibroblast Growth Factor 21 in Liver by Inhibition of Histone Deacetylase 3. Diabetes 61, 797–806.

Lieber, C.S., Leo, M.A., Mak, K.M., Xu, Y., Cao, Q., Ren, C., Ponomarenko, A., and DeCarli, L.M. (2004). Model of nonalcoholic steatohepatitis. Am J Clin Nutr 79, 502–509.

Listenberger, L.L., Han, X., Lewis, S.E., Cases, S., Farese, R.V., Ory, D.S., and Schaffer, J.E. (2003). Triglyceride accumulation protects against fatty acid-induced lipotoxicity. Proc. Natl. Acad. Sci. U.S.A. 100, 3077–3082.

Lodhi, I.J., Wei, X., and Semenkovich, C.F. (2011). Lipoexpediency: de novo lipogenesis as a metabolic signal transmitter. Trends Endocrinol Metab 22, 1–8.

Ludwig, J., Viggiano, T.R., McGill, D.B., and Oh, B.J. (1980). Nonalcoholic steatohepatitis: Mayo Clinic experiences with a hitherto unnamed disease. Mayo Clin. Proc. 55, 434–438.

Ma, D.W.L., Arendt, B.M., Hillyer, L.M., Fung, S.K., McGilvray, I., Guindi, M., and Allard, J.P. (2016). Plasma phospholipids and fatty acid composition differ between liver biopsy-proven nonalcoholic fatty liver disease and healthy subjects. Nutr Diabetes 6, e220.

Malik, A.N., Shahni, R., Rodriguez-de-Ledesma, A., Laftah, A., and Cunningham, P. (2011). Mitochondrial DNA as a non-invasive biomarker: Accurate quantification using real time quantitative PCR without co-amplification of pseudogenes and dilution bias. Biochemical and Biophysical Research Communications 412, 1–7.

McGarry, J.D., Leatherman, G.F., and Foster, D.W. (1978). Carnitine palmitoyltransferase I. The site of inhibition of hepatic fatty acid oxidation by malonyl-CoA. J. Biol. Chem. 253, 4128–4136.

Mu, H., and Høy, C.-E. (2004). The digestion of dietary triacylglycerols. Prog. Lipid Res. 43, 105–133.

Niot, I., Poirier, H., Tran, T.T.T., and Besnard, P. (2009). Intestinal absorption of long-chain fatty acids: Evidence and uncertainties. Progress in Lipid Research 48, 101–115.

Phillips, N.R., Sprouse, M.L., and Roby, R.K. (2014). Simultaneous quantification of mitochondrial DNA copy number and deletion ratio: A multiplex real-time PCR assay. Scientific Reports 4.

Pogribny, I.P., Tryndyak, V.P., Bagnyukova, T.V., Melnyk, S., Montgomery, B., Ross, S.A., Latendresse, J.R., Rusyn, I., and Beland, F.A. (2009). Hepatic epigenetic phenotype predetermines individual susceptibility to hepatic steatosis in mice fed a lipogenic methyl-deficient diet. J Hepatol 51, 176–186.

Poirier, Y., Antonenkov, V.D., Glumoff, T., and Hiltunen, J.K. (2006). Peroxisomal β-oxidation—A metabolic pathway with multiple functions. Biochimica et Biophysica Acta (BBA) - Molecular Cell Research 1763, 1413–1426.

Potthoff, M.J., Inagaki, T., Satapati, S., Ding, X., He, T., Goetz, R., Mohammadi, M., Finck, B.N., Mangelsdorf, D.J., Kliewer, S.A., et al. (2009). FGF21 induces PGC-1α and regulates carbohydrate and fatty acid metabolism during the adaptive starvation response. PNAS 106, 10853–10858.

Puri, P., Baillie, R.A., Wiest, M.M., Mirshahi, F., Choudhury, J., Cheung, O., Sargeant, C., Contos, M.J., and Sanyal, A.J. (2007). A lipidomic analysis of nonalcoholic fatty liver disease. Hepatology 46, 1081–1090.

Puri, P., Wiest, M.M., Cheung, O., Mirshahi, F., Sargeant, C., Min, H.-K., Contos, M.J., Sterling, R.K., Fuchs, M., Zhou, H., et al. (2009). The plasma lipidomic signature of nonalcoholic steatohepatitis. Hepatology 50, 1827–1838.

Rakhshandehroo, M., Hooiveld, G., Müller, M., and Kersten, S. (2009). Comparative Analysis of Gene Regulation by the Transcription Factor PPARα between Mouse and Human. PLOS ONE 4, e6796.

Raso, G.M., Simeoli, R., Russo, R., Iacono, A., Santoro, A., Paciello, O., Ferrante, M.C., Canani, R.B., Calignano, A., and Meli, R. (2013). Effects of Sodium Butyrate and Its Synthetic Amide Derivative on Liver Inflammation and Glucose Tolerance in an Animal Model of Steatosis Induced by High Fat Diet. PLOS ONE 8, e68626.

Renaud, H.J., Cui, J.Y., Lu, H., and Klaassen, C.D. (2014). Effect of Diet on Expression of Genes Involved in Lipid Metabolism, Oxidative Stress, and Inflammation in Mouse Liver–Insights into Mechanisms of Hepatic Steatosis. PLOS ONE 9, e88584.

Ricchi, M., Odoardi, M.R., Carulli, L., Anzivino, C., Ballestri, S., Pinetti, A., Fantoni, L.I., Marra, F., Bertolotti, M., Banni, S., et al. (2009). Differential effect of oleic and palmitic acid on lipid accumulation and apoptosis in cultured hepatocytes. J. Gastroenterol. Hepatol. 24, 830–840.

Romestaing, C., Piquet, M.-A., Bedu, E., Rouleau, V., Dautresme, M., Hourmand-Ollivier, I., Filippi, C., Duchamp, C., and Sibille, B. (2007). Long term highly saturated fat diet does not induce NASH in Wistar rats. Nutr Metab (Lond) 4, 4.

Rustan, A.C., and Drevon, C.A. (2001). Fatty Acids: Structures and Properties. In eLS, (John Wiley & Sons, Ltd), p.

Schaffer, J.E., and Lodish, H.F. (1994). Expression cloning and characterization of a novel adipocyte long chain fatty acid transport protein. Cell 79, 427–436.

Sharma, S., and Black, S.M. (2009). CARNITINE HOMEOSTASIS, MITOCHONDRIAL FUNCTION, AND CARDIOVASCULAR DISEASE. Drug Discov Today Dis Mech 6, e31–e39.

Shokolenko, I., Venediktova, N., Bochkareva, A., Wilson, G.L., and Alexeyev, M.F. (2009). Oxidative stress induces degradation of mitochondrial DNA. Nucleic Acids Res 37, 2539–2548.

Soardo, G., Donnini, D., Domenis, L., Catena, C., De Silvestri, D., Cappello, D., Dibenedetto, A., Carnelutti, A., Bonasia, V., Pagano, C., et al. (2011). Oxidative stress is activated by free fatty acids in cultured human hepatocytes. Metab Syndr Relat Disord 9, 397–401.

Soma, M.R., Mims, M.P., Chari, M.V., Rees, D., and Morrisett, J.D. (1992). Triglyceride metabolism in 3T3-L1 cells. An in vivo 13C NMR study. J. Biol. Chem. 267, 11168–11175.

Song, S., Zhang, Y., Ma, K., Jackson-Hayes, L., Lavrentyev, E.N., Cook, G.A., Elam, M.B., and Park, E.A. (2004). Peroxisomal proliferator activated receptor gamma coactivator (PGC-1α) stimulates carnitine palmitoyltransferase I (CPT-Iα) through the first intron. Biochimica et Biophysica Acta (BBA) - Gene Structure and Expression 1679, 164–173.

Song, S., Attia, R.R., Connaughton, S., Niesen, M.I., Ness, G.C., Elam, M.B., Hori, R.T., Cook, G.A., and Park, E.A. (2010). Peroxisome proliferator activated receptor α (PPARα) and PPAR gamma coactivator (PGC-1α) induce carnitine palmitoyltransferase IA (CPT-1A) via independent gene elements. Mol Cell Endocrinol 325, 54–63.

Szklarczyk, D., Franceschini, A., Wyder, S., Forslund, K., Heller, D., Huerta-Cepas, J., Simonovic, M., Roth, A., Santos, A., Tsafou, K.P., et al. (2015). STRING v10: protein-protein interaction networks, integrated over the tree of life. Nucleic Acids Res. 43, D447-452.

Takahashi, Y., Soejima, Y., and Fukusato, T. (2012). Animal models of nonalcoholic fatty liver disease/nonalcoholic steatohepatitis. World J Gastroenterol 18, 2300–2308.

Talayero, B.G., and Sacks, F.M. (2011). The Role of Triglycerides in Atherosclerosis. Curr Cardiol Rep 13, 544–552.

Turrens, J.F. (2003). Mitochondrial formation of reactive oxygen species. J Physiol 552, 335–344.

Wang, C., Tao, Q., Wang, X., Wang, X., and Zhang, X. (2016). Impact of high-fat diet on liver genes expression profiles in mice model of nonalcoholic fatty liver disease. Environmental Toxicology and Pharmacology 45, 52–62.

Xu, Q., Chen, S.Y., Deng, L.D., Feng, L.P., Huang, L.Z., and Yu, R.R. (2013). Antioxidant effect of mogrosides against oxidative stress induced by palmitic acid in mouse insulinoma NIT-1 cells. Braz J Med Biol Res 46, 949–955.

Youle, R.J., and van der Bliek, A.M. (2012). Mitochondrial Fission, Fusion, and Stress. Science 337, 1062–1065.

Younossi, Z.M., Koenig, A.B., Abdelatif, D., Fazel, Y., Henry, L., and Wymer, M. (2016). Global epidemiology of nonalcoholic fatty liver disease-Meta-analytic assessment of prevalence, incidence, and outcomes. Hepatology 64, 73–84.

BIOGRAPHY

Peter Masschelin graduated from W. T. Woodson High School, Fairfax, Virginia, in 2009. He received his Bachelor of Science from Allegheny College in 2014.